PHYSICAL REVIEW D **89,** 114019 (2014)

Phenomenological study of the $B_c \to BP, BV$ decays with perturbative QCD approach

Junfeng Sun, Yueling Yang,* Qin Chang,† and Gongru Lu

Institute of Particle and Nuclear Physics, Henan Normal University, Xinxiang 453007, China

(Received 6 April 2014; published 18 June 2014)

Inspired by the recent LHCb measurements and forthcoming great potential on B_c meson, we study the exclusive $B_c \to B_q P$, $B_q V$ decays with the perturbative QCD approach, where $q = u$, d, s and P and V denote the lightest pseudoscalar and vector $SU(3)$ nonet meson, respectively. By retaining the quark transverse momentum, employing the Sudakov factors, and choosing the typical scale as the maximum virtualities of the internal particles, we calculate the $B_c \to B$ transition from factors, and our results show that about 90% of the contribution to form factors comes from the $\alpha_s/\pi < 0.3$ region. The contributions of penguin and annihilation to branching ratios are very small due to the serious suppression by the CKM factors. There are some hierarchy relations among the $B_c \to BP$, BV decays. The branching ratios for $B_c \to B_{d,s}\pi$, $B_{d,s}\rho$, $B_s K$ are large and could be measured by the running LHCb.

DOI: 10.1103/PhysRevD.89.114019 PACS numbers: 14.40.Nd, 13.25.Hw

I. INTRODUCTION

The B_c meson is the heaviest ground pseudoscalar meson with explicit both bottom and charm flavor. The yield ratio of the B_c meson is very small [1], but it is still possible to obtain enough measurements to explore its property at high-energy colliders. The B_c meson was observed for the first time via the semileptonic decay $B_c \to J/\psi \ell \nu$ in 1.8 TeV $p\bar{p}$ collisions using the CDF detector at the Fermilab Tevatron in 1998 [2]. Recently, its mass has been accurately determined at the $\mathcal{O}(10^{-4})$ level from the fully reconstructed $B_c \to J/\psi\pi$ mode by the CDF and LHCb experimental groups [3,4], and its lifetime is also measured at the ~3% level by the LHCb Collaboration [5].

The B_c meson, laying below BD threshold, can decay only via the weak interaction. Its decay modes can be divided into three types [6,7]: (1) the c quark decays while the b quark as a spectator; (2) the b quark decays while the c quark as a spectator; (3) the annihilation channel. The c quark decay modes [the type (1)] are responsible for about 70% of the width of B_c meson [8]. This type of decay process, although very challenging to experiments, has recently been observed in the $B_c \to B_s\pi$ mode with significance in excess of 5 standard deviations by the LHCb Collaboration [9]. The b quark decay modes [the type (2)] account for about 20% of the width of the B_c meson [10]. The $b \to c$ transition offers a well-reconstructed experimental signature at the Tevatron and LHC, for example, in the decay modes of $B_c^+ \to J/\psi\pi^+$ [3,4,11], $\psi(2S)\pi^+$ [12], $J/\psi D_s^{(*)+}$ [13], $J/\psi K^+K^-\pi^+$ [14], $J/\psi\pi^+\pi^-\pi^+$ [15], $J/\psi e^+\nu_e$ [16] and so on. The weak annihilation mode [type (3)] is estimated to take 10% shares of the width of the B_c meson [10]. The pure weak annihilation decay to two light mesons, $B_c \to u + d$, is so highly helicity suppressed that there is little probability of detecting the charmless and/or bottomless hadronic decays $B_c \to PP$, PV, VV [17], where P and V denote the lightest $SU(3)$ pseudoscalar and vector mesons, respectively; and to date, no corresponding measurements exist.

It is estimated that one could expect $\mathcal{O}(10^{10})$ of the B_c mesons per year at the LHC [18]. Along with the running of the LHC, more and more B_c decay modes will be observed. Anticipating the experimental developments, many studies (see Table I) have been devoted to the bottom conserving and charm changing decay modes $B_c \to BP$, BV, including estimates undertaken within various quark models assisted by confining potential [19–23], with potential models based on the Bethe-Salpeter equation [7,24], with BSW or ISGW models [6,25], with QCD sum rules [18], with heavy quark spin symmetry [26], with QCD factorization at the leading order [27], but without perturbative QCD (pQCD) approach. In this paper, we study the $B_c \to BP$, BV decays with the pQCD approach [28] to fill in this gap and provide a ready reference to the existing and forthcoming experiments.

This paper is organized as follows: In Sec. II, we discuss the theoretical framework, compute the $B_c \to B$ transition form factors and the amplitudes for $B_c \to BP$, BV decays with the pQCD approach. Section III is devoted to the numerical results. Finally, we summarize in Sec. IV.

II. THEORETICAL FRAMEWORK AND THE DECAY AMPLITUDES

A. The effective Hamiltonian

Because of the hierarchy $m_{W^\pm} \gg m_{b,c} \gg \Lambda_{\rm QCD}$ (where $m_{W^\pm}$ and $m_{b,c}$ are the mass of the $W^\pm$ boson and b, c quarks, respectively; $\Lambda_{\rm QCD}$ is the QCD confinement scale), one typically use the effective field theory to deal with

*yangyueling@htu.cn
†changqin@htu.cn

TABLE I. Branching ratios of $B_c \to BP$, BV decays with the fixed coefficients $a_1 = 1.20$ and $a_2 = -0.317$, and form factors $F_0^{B_c \to B_q}(0)$.

Reference	[19][a]	[20][b]	[27][c]	[21][d]	[22][e]	[23][f]	[18][g]	[26][h]	[25][i]	[7][j]	[24][k]	[6][l]
$F_0^{B_c \to B}(0)$	1.01	0.467 (0.426)	0.8	0.39	0.58	0.39	1.27	0.66	0.831			
$F_0^{B_c \to B_s}(0)$	1.03	0.573 (0.571)	0.8	0.58	0.61	0.50	1.3	0.66	0.859			
$\mathcal{B}r(B_c^+ \to B_s^0 \pi^+)$	10.9×10^{-2}	$3.72\ (3.70) \times 10^{-2}$	5.31×10^{-2}	3.51×10^{-2}	3.9×10^{-2}	2.52×10^{-2}	16.4×10^{-2}	3.03×10^{-2}	7.85×10^{-2}	5.79×10^{-2}	1.57×10^{-2}	$3.08\ (4.36) \times 10^{-2}$
$\mathcal{B}r(B_c^+ \to B_s^0 \rho^+)$	9.05×10^{-2}	$2.56\ (2.34) \times 10^{-2}$	6.27×10^{-2}	2.34×10^{-2}	2.3×10^{-2}	1.41×10^{-2}	7.2×10^{-2}	1.35×10^{-2}	4.70×10^{-2}	4.44×10^{-2}	3.88×10^{-2}	$1.24\ (2.00) \times 10^{-2}$
$\mathcal{B}r(B_c^+ \to B_s^0 K^+)$	7.23×10^{-3}	$2.87\ (2.84) \times 10^{-3}$	3.68×10^{-3}	2.9×10^{-3}	2.9×10^{-3}	2.1×10^{-3}	1.06×10^{-2}	2.13×10^{-3}	5.71×10^{-3}	4.16×10^{-3}	1.68×10^{-3}	$2.16\ (3.25) \times 10^{-3}$
$\mathcal{B}r(B_c^+ \to B_s^0 K^{*+})$	3.4×10^{-4}	$6.9\ (6.1) \times 10^{-5}$	1.65×10^{-3}	1.3×10^{-4}	1.1×10^{-4}	3.0×10^{-5}		4.26×10^{-5}	2.36×10^{-4}	2.93×10^{-3}	1.05×10^{-3}	
$\mathcal{B}r(B_c^+ \to B_d^0 \pi^+)$	7.2×10^{-3}	$1.57\ (1.31) \times 10^{-3}$	3.73×10^{-3}	1.1×10^{-3}	2.0×10^{-3}	1.0×10^{-3}	1.06×10^{-2}	1.95×10^{-3}	5.35×10^{-3}	3.27×10^{-3}	1.02×10^{-3}	$0.96\ (1.87) \times 10^{-3}$
$\mathcal{B}r(B_c^+ \to B_d^0 \rho^+)$	1.18×10^{-2}	$1.95\ (1.52) \times 10^{-3}$	5.27×10^{-3}	1.4×10^{-3}	2.0×10^{-3}	1.3×10^{-3}	9.6×10^{-3}	1.53×10^{-3}	5.98×10^{-3}	5.92×10^{-3}	2.78×10^{-3}	$0.93\ (2.12) \times 10^{-3}$
$\mathcal{B}r(B_c^+ \to B_d^0 K^+)$	5.4×10^{-4}	$1.3\ (1.1) \times 10^{-4}$	2.66×10^{-4}	1.0×10^{-4}	1.5×10^{-4}	9.0×10^{-5}	7.0×10^{-4}	1.39×10^{-4}		2.53×10^{-4}	1.04×10^{-4}	
$\mathcal{B}r(B_c^+ \to B_d^0 K^{*+})$	2.9×10^{-4}	$4.2\ (3.2) \times 10^{-5}$	2.26×10^{-4}	3.9×10^{-5}	4.8×10^{-5}	4.0×10^{-5}	1.5×10^{-4}	3.17×10^{-5}		1.78×10^{-4}	1.24×10^{-4}	
$\mathcal{B}r(B_c^+ \to B_u^+ \bar{K}^0)$	1.26×10^{-2}	$3.36\ (2.79) \times 10^{-3}$	2.21×10^{-5}	2.5×10^{-3}	3.8×10^{-3}	2.4×10^{-3}	1.98×10^{-2}		1.72×10^{-2}	6.67×10^{-3}	2.70×10^{-3}	$1.95\ (4.25) \times 10^{-3}$
$\mathcal{B}r(B_c^+ \to B_u^+ \bar{K}^{*0})$	7.1×10^{-3}	$1.08\ (0.80) \times 10^{-3}$	1.84×10^{-5}	9.3×10^{-4}	1.1×10^{-3}	9.0×10^{-4}	4.3×10^{-3}		6.30×10^{-3}	4.72×10^{-3}	3.24×10^{-3}	$0.69\ (1.67) \times 10^{-3}$
$\mathcal{B}r(B_c^+ \to B_u^+ \pi^0)$	2.5×10^{-4}	$5.5\ (4.6) \times 10^{-5}$	4.51×10^{-7}	3.8×10^{-5}	7.0×10^{-5}	4.0×10^{-5}	3.7×10^{-4}		3.23×10^{-4}	1.14×10^{-4}	3.53×10^{-5}	$3.32\ (6.57) \times 10^{-5}$
$\mathcal{B}r(B_c^+ \to B_u^+ \rho^0)$	4.1×10^{-4}	$6.8\ (5.3) \times 10^{-5}$	6.48×10^{-7}	5.0×10^{-5}	7.1×10^{-5}	5.0×10^{-5}	3.4×10^{-4}		3.59×10^{-4}	2.06×10^{-4}	9.68×10^{-5}	$3.25\ (7.40) \times 10^{-5}$
$\mathcal{B}r(B_c^+ \to B_u^+ \omega)$		$5.1\ (3.9) \times 10^{-5}$	5.82×10^{-7}						3.36×10^{-4}			$2.63\ (6.02) \times 10^{-5}$
$\mathcal{B}r(B_c^+ \to B_u^+ \eta)$		$2.8\ (2.3) \times 10^{-4}$	1.61×10^{-6}									
$\mathcal{B}r(B_c^+ \to B_u^+ \eta')$		$3.8\ (3.2) \times 10^{-6}$	8.77×10^{-8}									
$\mathcal{B}r(B_c^+ \to B_u^+ K^0)$		$8.8\ (7.3) \times 10^{-6}$	6.54×10^{-8}									
$\mathcal{B}r(B_c^+ \to B_u^+ K^{*0})$		$2.8\ (2.1) \times 10^{-6}$	5.47×10^{-8}									

[a]It is estimated in the relativistic independent quark model based on the scalar-vector form confining potential.
[b]It is estimated in the light-front quark model using the Coulomb plus linear confining (harmonic oscillator) potential.
[c]It is estimated at the leading order in the QCD factorziation approach with Wilson coefficients $c_1 = 1.22$ and $c_2 = -0.42$.
[d]It is estimated in the nonrelativistic constituent quark model using the Coulomb plus confining potential.
[e]It is estimated in the relativistic constituent quark model.
[f]It is estimated in the relativistic constituent quark model.
[g]It is estimated in the QCD sum rules.
[h]It is estimated in the constituent quark model.
[i]It is estimated in the BSW model with $\omega = 0.8$ GeV.
[j]It is estimated in the potential model based on the Bethe-Salpeter equation.
[k]It is estimated in the relativistic model based on the Bethe-Salpeter equation.
[l]It is estimated in the BSW (ISGW) model.

weak decays of the hadron containing heavy quark. Using the operator product expansion, the low energy effective Hamiltonian relevant to nonleptonic $B_c \to BP, BV$ decays can be written as [29]

$$\mathcal{H}_{\rm eff} = \frac{G_F}{\sqrt{2}}\Big\{ V_{ub}V_{cb}^*[C_1^a(\mu)Q_1^a(\mu) + C_2^a(\mu)Q_2^a(\mu)] + \sum_{q_1,q_2} V_{uq_1}V_{cq_2}^*[C_1(\mu)Q_1(\mu) + C_2(\mu)Q_2(\mu)] + \sum_{q_3}\sum_{k=3}^{10} V_{uq_3}V_{cq_3}^* C_k(\mu)Q_k(\mu)\Big\} + \text{H.c.}, \quad (1)$$

where G_F is the Fermi coupling constant; q_i denotes the down-type quarks d and s. The Wilson coefficients $C_i(\mu)$ summarize the contributions from scales higher than μ, which are calculable and can be evaluated to the scale μ with the renormalization group equation. Their numerical values at four different scales μ are listed in Table. II. The expressions of the local four-quark operators Q_i can be written explicitly as follows:

(i) current-current (tree) operators

$$Q_1^a = (\bar{b}_\alpha c_\alpha)_{V-A}(\bar{u}_\beta b_\beta)_{V-A}, \quad (2)$$

$$Q_2^a = (\bar{b}_\alpha c_\beta)_{V-A}(\bar{u}_\beta b_\alpha)_{V-A}, \quad (3)$$

$$Q_1 = (\bar{q}_{2\alpha} c_\alpha)_{V-A}(\bar{u}_\beta q_{1\beta})_{V-A}, \quad (4)$$

$$Q_2 = (\bar{q}_{2\alpha} c_\beta)_{V-A}(\bar{u}_\beta q_{1\alpha})_{V-A}, \quad (5)$$

(ii) QCD penguin operators

$$Q_3 = \sum_q (\bar{u}_\alpha c_\alpha)_{V-A}(\bar{q}_\beta q_\beta)_{V-A}, \quad (6)$$

$$Q_4 = \sum_q (\bar{u}_\alpha c_\beta)_{V-A}(\bar{q}_\beta q_\alpha)_{V-A}, \quad (7)$$

$$Q_5 = \sum_q (\bar{u}_\alpha c_\alpha)_{V-A}(\bar{q}_\beta q_\beta)_{V+A}, \quad (8)$$

TABLE II. Numerical values of Wilson coefficients at different scales.

μ	1 GeV	m_c	2 GeV	m_b
C_1	1.294	1.230	1.156	1.087
$C_2 \times 10$	−5.327	−4.370	−3.177	−1.947
$C_3 \times 10^2$	4.764	3.639	2.471	1.482
$C_4 \times 10^2$	−9.674	−7.731	−5.602	−3.605
$C_5 \times 10^3$	7.009	9.963	10.55	8.613
$C_6 \times 10^2$	−15.50	−11.31	−7.339	−4.240
$C_7 \times 10^5$	−7.465	−11.53	−10.98	0.4438
$C_8 \times 10^3$	1.660	1.205	0.7759	0.4491
$C_9 \times 10^2$	−1.213	−1.149	−1.078	−1.009
$C_{10} \times 10^3$	5.493	4.474	3.287	2.131

$$Q_6 = \sum_q (\bar{u}_\alpha c_\beta)_{V-A}(\bar{q}_\beta q_\alpha)_{V+A}, \quad (9)$$

(iii) electroweak penguin operators

$$Q_7 = \sum_q \frac{3}{2} Q_q (\bar{u}_\alpha c_\alpha)_{V-A}(\bar{q}_\beta q_\beta)_{V+A}, \quad (10)$$

$$Q_8 = \sum_q \frac{3}{2} Q_q (\bar{u}_\alpha c_\beta)_{V-A}(\bar{q}_\beta q_\alpha)_{V+A}, \quad (11)$$

$$Q_9 = \sum_q \frac{3}{2} Q_q (\bar{u}_\alpha c_\alpha)_{V-A}(\bar{q}_\beta q_\beta)_{V-A}, \quad (12)$$

$$Q_{10} = \sum_q \frac{3}{2} Q_q (\bar{u}_\alpha c_\beta)_{V-A}(\bar{q}_\beta q_\alpha)_{V-A}, \quad (13)$$

where the tree operators of $Q_{1,2}^q$ describe the weak annihilation topology; α and β are the color indices; the q in penguin operators denotes all the active quarks at scale $\mu = \mathcal{O}(m_c)$, i.e., $q = u, d, s, c$; the left- and right-handed currents are defined as $(\bar{q}_\alpha q'_\beta)_{V\pm A} \equiv \bar{q}_\alpha \gamma_\mu (1 \pm \gamma_5) q'_\beta$; and Q_q is the charge of quark q in the unit of $|e|$.

B. Hadronic matrix elements

The essential problem obstructing the calculation of decay amplitude is how to properly evaluate the hadronic matrix elements of the local operators. Using the Brodsky-Lepage approach [30], the hadronic matrix elements can be written as the convolution of a hard-scattering kernels containing perturbative QCD contributions with the universal wave functions reflecting the nonperturbative dynamics. Currently, there are three popular phenomenological approaches to evaluate the hadronic matrix elements as an expansion in the strong coupling constant α_s and in the ratio $\Lambda_{\rm QCD}/m_Q$, which are entitled to QCD factorization (QCDF) [31], the soft-collinear effective theory (SCET) [32], and the pQCD approach [28]. These methods differ from each other in several aspects. For example, only the collinear degrees of freedom are taken into account in QCDF and SCET, while the transverse momenta implemented with the help of the Sudakov formalism in pQCD approach. The other different features of these methods are power counting, the choice of the scale at which the strong interaction effects are calculated, how to deal with the contribution of spectator scattering and weak annihilation, and so on. With the running LHCb and the advent of SuperKEKB physics program, the precision of observables will be greatly improved, and it should be possible to disentangle the underlying dynamics in nonleptonic B decays.

In this paper, we study the $B_c \to BP, BV$ decays with the pQCD approach. By keeping the parton transverse momentum and employing the Sudakov factors to modify the

endpoint behavior, the hadron matrix elements are expressed as the convolution of wave functions and the heavy quark decay subamplitudes, integrated over the longitudinal and transverse momenta. After the Fourier transformation, the typical formula of the hadron matrix elements can be written as

$$M \propto \int \mathbf{d}x_1\mathbf{d}x_2\mathbf{d}x_3 \int \mathbf{d}\vec{b}_1\mathbf{d}\vec{b}_2\mathbf{d}\vec{b}_3\phi_{B_c}(x_1,\vec{b}_1)\phi_{B_q}(x_2,\vec{b}_2) \times \phi_{P,V}(x_3,\vec{b}_3)e^{-S_{B_c}(t)-S_{B_q}(t)-S_{P,V}(t)}H(x_i,\vec{b}_i,t), \quad (14)$$

where ϕ_i is the meson wave functions; $\vec{b}_i$ is the conjugate variable of the transverse moment $\vec{k}_{i\perp}$ of valence quark; $e^{-S_i(t)}$ is the Sudakov factor; and H is the process-dependent heavy quark decay subamplitudes. The kinematic variables and wave functions are given as below.

C. Kinematic variables

In the terms of the light cone coordinate, the momenta of the valence quarks and hadrons in the rest frame of the B_c meson are defined as

$$p_1 = \frac{m_1}{\sqrt{2}}(1,1,0), \quad (15)$$

$$p_2 = (q_2^+, q_2^-, 0), \quad (16)$$

$$p_3 = (q_3^-, q_3^+, 0), \quad (17)$$

$$k_i = x_i p_i + (0,0,\vec{k}_{i\perp}), \quad (18)$$

$$\epsilon_\parallel = \frac{1}{m_3}(-q_3^-, q_3^+, 0), \quad (19)$$

$$q_i^\pm = \frac{E_i \pm p}{\sqrt{2}}, \quad (20)$$

where the subscript $i = 1, 2, 3$ refers to B_c, B_q and the light meson, respectively; k_i, $\vec{k}_{i\perp}$, x_i are the momentum, transverse momentum, and longitudinal momentum fraction of light valence quark confined within the meson, respectively; and $\epsilon_\parallel$ denotes the longitudinal polarization vector of the light vector meson. E_i and p are the energy and the momentum of final state, respectively. For the sake of brevity, the Lorentz-invariant variables are defined by

$$s = 2p_2\cdot p_3, \qquad t = 2p_1\cdot p_2, \qquad u = 2p_1\cdot p_3. \quad (21)$$

D. Wave functions

In order to get the analytic formulas of the decay amplitudes, we use the light-cone wave functions which can be decomposed as [33]

$$\langle 0|\bar{b}_\alpha(0)c_\beta(z)|B_c(p_1)\rangle = \frac{-if_{B_c}}{4N_c}\int \mathbf{d}^4k_1\{e^{-ik_1\cdot z}\phi_{B_c}(\not{p}_1 + m_{B_c})\gamma_5\}_{\beta\alpha}, \quad (22)$$

$$\langle B_q(p_2)|\bar{q}_\alpha(z)b_\beta(0)|0\rangle = \frac{-if_{B_q}}{4N_c}\int \mathbf{d}^4k_2\{e^{+ik_2\cdot z}\phi_{B_q}\gamma_5(\not{p}_2 + m_{B_q})\}_{\beta\alpha}, \quad (23)$$

$$\langle P(p_3)|\bar{q}_{1\alpha}(z)q_{2\beta}(0)|0\rangle = \frac{-if_P}{4N_c}\int \mathbf{d}^4k_3 e^{+ik_3\cdot z} \times \{\gamma_5[\not{p}_3\phi_P^a + \mu_P\phi_P^p + \mu_P(\not{n}_-\not{n}_+ - 1)\phi_P^t]\}_{\beta\alpha}, \quad (24)$$

$$\langle V(p_3,\epsilon_\parallel)|\bar{q}_{1\alpha}(z)q_{2\beta}(0)|0\rangle = \frac{f_V}{4N_c}\int \mathbf{d}^4k_3 \mathrm{e}^{+ik_2\cdot z} \times \left\{\not{\epsilon}_\parallel\left[m_V\phi_V + \not{p}_3\frac{f_V^T}{f_V}\phi_V^t\right] + \frac{m_V f_V^T}{f_V}\phi_V^s\right\}_{\beta\alpha}, \quad (25)$$

where $N_c = 3$ is the color number; f_i is the decay constant. The explicit expressions of the light-cone distribution amplitudes (ϕ_{B_c}, ϕ_{B_q}, $\phi_P^{a,p,t}$,ϕ_V and $\phi_V^{t,s}$) are collected in Appendix A and B.

E. Form factor

The $B_c \to B_q$ form factors are defined as [34]

$$\langle B_q(p_2)|(\bar{q}c)_{V-A}^\mu|B_c(p_1)\rangle = \left\{(p_1+p_2)^\mu - \frac{m_1^2 - m_2^2}{q^2}q^\mu\right\} \times F_1 + \frac{m_1^2 - m_2^2}{q^2}q^\mu F_0, \quad (26)$$

where $q = p_1 - p_2$ is the momentum transfer. Usually, the longitudinal form factor $F_0(q^2)$ is compulsorily equal to the transverse form factor $F_1(q^2)$ in the largest recoil limit to cancel singularities appearing at the pole $q^2 = 0$, i.e., $F_0(0) = F_1(0)$.

The $B_c \to B$ transition form factors can be written as the convolution of wave functions and the one-gluon exchange scattering amplitudes using the pQCD approach. There are two types of diagrams contributing to the $B_c \to B$ transition form factors, which are displayed in Fig. 1. The expression of the form factors is written as

$$F_1(q^2) = \frac{\pi C_F}{N_c}f_{B_c}f_{B_q}\int_0^1 \mathbf{d}x_1\mathbf{d}x_2 \times \int_0^\infty \mathbf{d}b_1\mathbf{d}b_2\phi_{B_c}(x_1)\phi_{B_q}(x_2,b_2) \times \{H_a[\{m_1(2m_2 - m_1) + q^2\}x_2 + m_c(2m_1 - m_2) - q^2] + H_b[\{m_2(2m_1 - m_2) + q^2\}x_1 - q^2]\}, \quad (27)$$

$$F_0(q^2) = \frac{\pi C_F}{N_c} f_{B_c} f_{B_q} \int_0^1 \mathbf{d}x_1 \mathbf{d}x_2 \int_0^\infty \mathbf{d}b_1 \mathbf{d}b_2 \phi_{B_c}(x_1) \phi_{B_q}(x_2, b_2)$$
$$\times \{H_a[\{(m_1 - m_2)^2 + m_2^2 - q^2\}x_2 + 2m_2(2m_1 - m_2) - m_c(2m_1 + m_2) + q^2]$$
$$- H_b[\{(m_1 - m_2)^2 + m_1^2 - q^2\}x_1 + 2m_1(2m_2 - m_1) + q^2]\} \frac{q^2}{m_1^2 - m_2^2} + F_1(q^2). \quad (28)$$

It is well known that the q^2-dependent behavior of the form factor is required in semileptonic B_c decays. To shed light on the momentum dependence, one needs a specific model to parameterize the form factors. Here we adopt the three-parameter form, i.e.,

$$F_i(q^2) = \frac{F_i(0)}{1 - \frac{q^2}{m^2} + \delta \frac{q^4}{m^4}}, \quad (29)$$

where the pole mass m and curvature parameter δ can be given by fit data of q^2-dependent form factors.

F. Decay amplitudes and branching ratios

There are generally eight diagrams (see Fig. 2) contributing to the $B_c \to BP, BV$ decays at the lowest order with the pQCD approach. For example, the amplitude of the $B_c \to B_s K$ decay can be written as

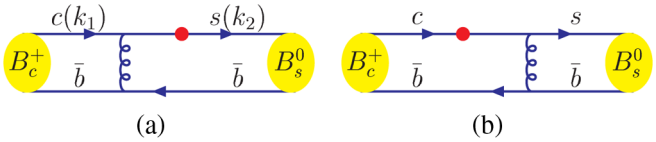

FIG. 1 (color online). The lowest order diagrams contributing to the $B_c \to B_s$ transition form factors, where the dot denotes an appropriate Dirac matrix.

$$\mathcal{A}(B_c^+ \to B_s^0 K^+) = V_{us} V_{cs}^* \{a_1 M_{ab,1}^P + C_2 M_{cd,1}^P\}$$
$$- V_{ub} V_{cb}^* \{(a_4 - a_{10}/2) M_{ab,1}^P$$
$$+ (a_6 - a_8/2) M_{ab,3}^P + (C_3 - C_9/2) M_{cd,1}^P$$
$$+ (C_5 - C_7/2) M_{cd,3}^P$$
$$- a_1 M_{ef,1}^P - C_2 M_{gh,1}^P\}, \quad (30)$$

where $V_{us}V_{cs}^*$ and $V_{ub}V_{cb}^*$ are the CKM factors; C_i are the Wilson coefficients; and the parameters a_i are defined as

$$a_i = C_i + C_{i+1}/N_c, \qquad (i = 1, 3, 5, 7, 9), \quad (31)$$

$$a_i = C_i + C_{i-1}/N_c, \qquad (i = 2, 4, 6, 8, 10). \quad (32)$$

The M_{ab}, M_{cd}, M_{ef}, M_{gh} denote the contributions of the factorizable emission diagrams [Figs. 2(a)–2(b)], the nonfactorizable emission diagrams [Figs. 2(c)–2(d)], the factorizable annihilation diagrams [Figs. 2(e)–2(f)], the nonfactorizable annihilation diagrams [Figs. 2(g)–2(h)], respectively. They are defined as

$$M_{ab,i}^{P,V} = M_{a,i}^{P,V} + M_{b,i}^{P,V}, \qquad M_{cd,i}^{P,V} = (M_{c,i}^{P,V} + M_{d,i}^{P,V})/N_c, \quad (33)$$

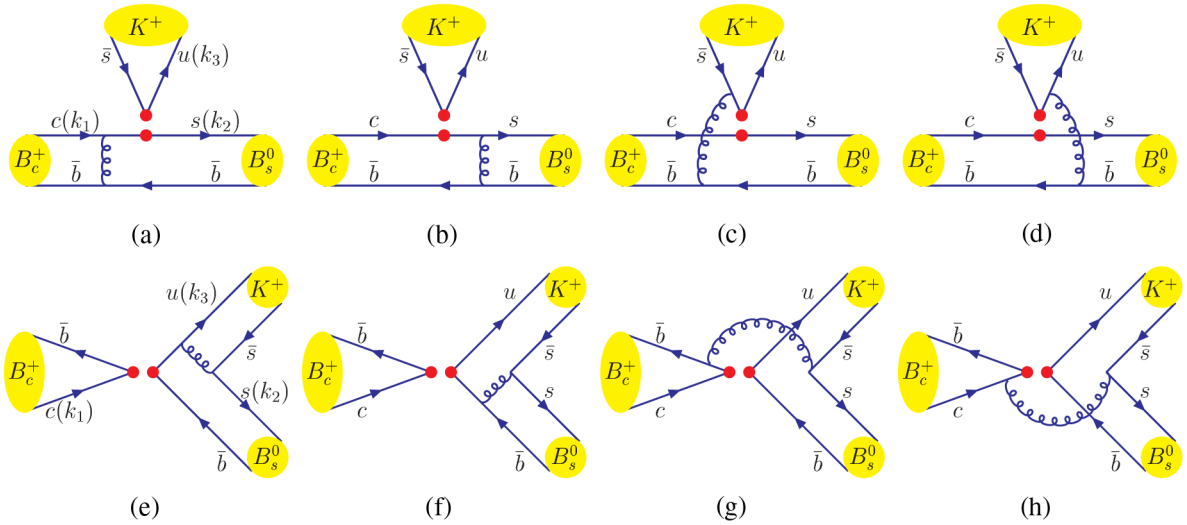

FIG. 2 (color online). Diagrams contributing to the $B_c \to B_s K$ decay, where (a) and (b) are called as the factorizable emission diagrams, (c) and (d) the nonfactorizable emission diagrams, (e) and (f) the factorizable annihilation diagrams, (g) and (h) the nonfactorizable annihilation diagrams.

$$M_{ef,i}^{P,V} = M_{e,i}^{P,V} + M_{f,i}^{P,V}, \qquad M_{gh,i}^{P,V} = (M_{g,i}^{P,V} + M_{h,i}^{P,V})/N_c. \tag{34}$$

Here the superscripts P and V on $M^{P,V}$ mean that the light final states are the pseudoscalar and vector mesons, respectively; the subscript i on $M_{i,j}$ corresponds to one index of Fig. 2; the subscript j on $M_{i,j}$ refers to one of three possible Dirac structures, namely $j = 1$ for $(V-A)\otimes(V-A)$, $j = 2$ for $(V-A)\otimes(V+A)$, and $j = 3$ for $-2(S-P)\otimes(S+P)$. The expressions of these building blocks $M_{i,j}^{k}$ of amplitudes are displayed in Appendix C. Our study shows that (i) for the factorizable topologies [Figs. 2(a), 2(b), 2(e), and 2(f)], the contribution of the color-singlet-current operators $(\bar{q}_{1\alpha}q_{2\alpha})_j(\bar{q}_{3\beta}q_{4\beta})_j$ is N_c times larger than that of the corresponding color-current operators $(\bar{q}_{1\alpha}q_{2\beta})_j(\bar{q}_{3\beta}q_{4\alpha})_j$, (ii) for the nonfactorizable topologies [Figs. 2(c), 2(d), 2(g), and 2(h)], the color-singlet-current operators contribute nothing, (iii) the nonfactorizable contributions corresponding to terms of both $M_{cd,i}^{P,V}$ and $M_{gh,i}^{P,V}$ are color-suppressed relative to the factorizable contributions corresponding to terms of both $M_{ab,i}^{P,V}$ and $M_{ef,i}^{P,V}$, and (iv) the nonfactorizable contributions might be important for the $B_c \to B_u P$, $B_u V$ decays, where term $M_{cd,1}^{P,V}$ is always multiplied by the large Wilson coefficient C_1.

As for the mixing of the physical states, η and η' meson, they are usually expressed as a linear combination of states in either an $SU(3)$ octet-singlet or quark-flavor mixing scheme. We will adopt the quark-flavor basis description proposed in [35], i.e.,

$$\begin{pmatrix} \eta \\ \eta' \end{pmatrix} = \begin{pmatrix} \cos\phi & -\sin\phi \\ \sin\phi & \cos\phi \end{pmatrix} \begin{pmatrix} \eta_q \\ \eta_s \end{pmatrix}, \tag{35}$$

where $\eta_q = (u\bar{u} + d\bar{d})/\sqrt{2}$ and $\eta_s = s\bar{s}$, respectively, and the mixing angle $\phi = (39.3 \pm 1.0)^\circ$ [35]. We assume that the distribution amplitudes of η_q and η_s are the same as those of the π meson, but with different decay constants and chiral parameters [35,36],

$$f_q = (1.07 \pm 0.02) f_\pi, \tag{36}$$

$$f_s = (1.34 \pm 0.06) f_\pi, \tag{37}$$

$$\mu_{\eta_q} = \frac{m_{\eta_q}^2}{m_u + m_d}, \tag{38}$$

$$\mu_{\eta_s} = \frac{m_{\eta_s}^2}{2m_s}, \tag{39}$$

$$m_{\eta_q}^2 = m_\eta^2 \cos^2\phi + m_{\eta'}^2 \sin^2\phi - \frac{\sqrt{2} f_s}{f_q}(m_{\eta'}^2 - m_\eta^2)\cos\phi\sin\phi, \tag{40}$$

$$m_{\eta_s}^2 = m_\eta^2 \sin^2\phi + m_{\eta'}^2 \cos^2\phi - \frac{f_q}{\sqrt{2} f_s}(m_{\eta'}^2 - m_\eta^2)\cos\phi\sin\phi. \tag{41}$$

The gluonic contributions are not considered in our calculation, because it is shown that (i) the fraction of gluonium contributions to η and η' is less than 15% [37] and (ii) the flavor-singlet contributions from the gluonic content of the $\eta^{(\prime)}$ meson is very small and can be neglected safely [38]. In addition, the contributions from the possible $c\bar{c}$ compositions of the $\eta^{(\prime)}$ meson are also not considered here.

In contrast, we assume the vector mesons are ideally mixed, i.e., the $\omega = (u\bar{u} + d\bar{d})/\sqrt{2}$ and $\phi = s\bar{s}$. In fact, the $B_c \to B\phi$ decay is forbidden by the kinematic constraint because the B_c meson is below the $B\phi$ threshold. So there are a total of seventeen $B_c \to BP$, BV decay modes. The decay amplitudes are listed in Appendix. D. The branching ratio in the B_c meson rest frame can be written as

$$\mathcal{B}r(B_c \to BM) = \frac{G_F^2 \tau_{B_c}}{16\pi} \frac{p}{m_{B_c}^2} |\mathcal{A}(B_c \to BM)|^2, \tag{42}$$

where the lifetime of the B_c meson is $\tau_{B_c} = 0.453 \pm 0.041$ ps [1].

III. NUMERICAL RESULTS AND DISCUSSIONS

The form factor and branching ratio depend on many parameters. To be specific, the parameters used in our calculation are listed in Table III. If not specified explicitly, we will take their central values as the default input. At the beginning of the calculation, we would like to claim that we have no intention to claim a precise prediction, but to provide an order of magnitude estimation in order to test the applicability of the pQCD approach for the $B_c \to BP$, BV decays.

Our numerical results on the form factors are given in Table IV, where the uncertainties come from the mass $m_b = 4.18 \pm 0.03$ GeV for b quark, $m_c = 1.275 \pm 0.025$ GeV for c quark, shape parameters of distribution amplitudes, i.e., $\omega_{B_c} = 0.50 \pm 0.05$ GeV for B_c meson, $\omega_{B_q} = 0.45 \pm 0.05 (0.55 \pm 0.05)$ GeV for $B_{u,d}$ (B_s) meson, and the typical scale $(1 \pm 0.1)t$, respectively.

There are some comments on the form factors.

(i) The isospin is a good symmetry for the form factor $F_{0,1}^{B_c \to B_u} = F_{0,1}^{B_c \to B_d}$, including the fitted pole mass m and curvature parameter δ. Considering the uncertainties, the values of form factors $F_{0,1}^{B_c \to B_q}$ at the pole $q^2 = 0$ are consistent with the recent results estimated with the relativistic independent quark model, where $F_{0,1}^{B_c \to B_{u,d}}(0) = 1.01$ and $F_{0,1}^{B_c \to B_s}(0) = 1.03$ [19]. As it is well known, the spectator is the heavy b quark in the $B_c \to B$ transition. The velocity of the

TABLE III. Numerical values of the input parameters.

Wolfenstein parameters	
$\lambda = 0.22535 \pm 0.00065$ [1]	$A = 0.811^{+0.022}_{-0.012}$ [1]
$\bar{\rho} = 0.131^{+0.026}_{-0.013}$ [1]	$\bar{\eta} = 0.345^{+0.013}_{-0.014}$ [1]
Masses of mesons and quarks	
$m_{B_u} = 5279.25 \pm 0.17$ MeV [1]	$m_{B_d} = 5279.58 \pm 0.17$ MeV [1]
$m_{B_s} = 5366.77 \pm 0.24$ MeV [1]	$m_{B_c} = 6.277 \pm 0.006$ GeV [1]
$m_c = 1.275 \pm 0.025$ GeV [1]	$m_b = 4.18 \pm 0.03$ GeV [1]
Decay constant of mesons	
$f_\pi = 130.41 \pm 0.20$ MeV [1]	$f_K = 156.1 \pm 0.8$ MeV [1]
$f_q = (1.07 \pm 0.02) f_\pi$ [35]	$f_s = (1.34 \pm 0.06) f_\pi$ [35]
$f_{B_{u,d}} = 190.5 \pm 4.2$ MeV [39]	$f_{B_s} = 227.7 \pm 4.5$ MeV [39]
$f_\rho = 216 \pm 3$ MeV [40]	$f_\rho^T(1\ \text{GeV}) = 165 \pm 9$ MeV [40]
$f_\omega = 187 \pm 5$ MeV [40]	$f_\omega^T(1\ \text{GeV}) = 151 \pm 9$ MeV [40]
$f_{K^*} = 220 \pm 5$ MeV [40]	$f_{K^*}^T(1\ \text{GeV}) = 185 \pm 10$ MeV [40]
$f_{B_c} = 489 \pm 4 \pm 3$ MeV [41]	$f_{3P}(1\ \text{GeV}) = (4.5 \pm 1.5) \times 10^{-3}\ \text{GeV}^2$ [42]
Gegenbauer moments[a] at the scale $\mu = 1$ GeV.	
$a^{\parallel}_{1,\rho} = 0$ [40]	$a^{\parallel}_{2,\rho} = 0.15 \pm 0.07$ [40]
$a^{\parallel}_{1,K^*} = 0.03 \pm 0.02$ [40]	$a^{\parallel}_{2,K^*} = 0.11 \pm 0.09$ [40]
$a^{\pi}_1 = 0$ [42]	$a^{\pi}_2 = 0.25 \pm 0.15$ [42]
$a^{K}_1 = 0.06 \pm 0.03$ [42]	$a^{K}_2 = 0.25 \pm 0.15$ [42]
$\omega^{\pi}_3 = -1.5 \pm 0.7$ [42]	$\omega^{K}_3 = -1.2 \pm 0.7$ [42]

[a]We will take the approximation $a_i^{\eta_q} = a_i^{\eta_s} = a_i^{\pi}$, and $a^{\parallel}_{i,\omega} = a^{\parallel}_{i,\rho}$.

B meson is very low in the rest frame of the B_c meson. The wave functions of B_c and B mesons overlap severely, which result in the large $B_c \to B$ transition form factors.

(ii) The q^2 dependence of the form factor is displayed in Fig. 3. From Eq. (28), we can see that the interference between Figs. 1(a) and 1(b) is destructive to $F_0(q^2) - F_1(q^2)$, so the shape line of $F_0(q^2)$ via q^2 should be close to that of $F_1(q^2)$. The shape lines will go up slowly at the beginning part, due to that with the increasing q^2, the velocity of the B meson become much low which leads to serious overlap between the wave functions of B_c and B_q mesons. But the shape lines will go down for large q^2, because the form factor $F_1(q^2)$ reduces with increasing q^2 [see Eq. (27)].

(iii) The form factors are sensitive to the choice of the shape parameter ω_{B_q} and the scale. In addition, the uncertainties from the decay constants of f_{B_c} and f_{B_q} are small, about 1% and 2%, respectively.

(iv) The contributions to form factor $F_0^{B_c \to B_s}(0)$ from different region of α_s/π is displayed in Fig. 4, where $e^{-S} \neq 1 (= 1)$ denote results with (without) the Sudakov factor; b_i is the conjugate variable of the transverse moment $k_{i\perp}$; α [see Eq. (C48)] and β [see Eq. (C50) and Eq. (C51)] are the virtuality of the internal gluon and quark, respectively. From Fig. 4(a) we can see that if one choose the virtuality of the internal gluon and quark as the typical scale, the contribution to form factor from $\alpha_s/\pi < 0.3$ region is less than 40%, that is to say, the hard and soft

TABLE IV. Form factor and the fitted parameters, where the uncertainties are from mass m_b, m_c, shape parameters ω_{B_c}, ω_{B_q} and typical scale t, respectively.

	$F_0(0)$	$1.074^{+0.007+0.016+0.031+0.172+0.131}_{-0.006-0.017-0.028-0.150-0.056}$	$F_1(0)$	$1.074^{+0.007+0.016+0.031+0.172+0.131}_{-0.006-0.017-0.028-0.150-0.056}$
$B_c \to B_u$	m	$1.123^{+0.003+0.001+0.010+0.040+0.021}_{-0.002-0.001-0.010-0.037-0.013}$	m	$1.110^{+0.004+0.011+0.014+0.007+0.022}_{-0.002-0.009-0.014-0.005-0.008}$
	δ	$2.689^{+0.040+0.212+0.104+0.858+0.358}_{-0.027-0.185-0.103-0.658-0.743}$	δ	$1.830^{+0.029+0.092+0.082+0.350+0.251}_{-0.022-0.084-0.083-0.309-0.564}$
	$F_0(0)$	$1.075^{+0.006+0.016+0.031+0.172+0.131}_{-0.007-0.017-0.028-0.150-0.056}$	$F_1(0)$	$1.075^{+0.006+0.016+0.031+0.172+0.131}_{-0.007-0.017-0.028-0.150-0.056}$
$B_c \to B_d$	m	$1.123^{+0.002+0.000+0.009+0.039+0.022}_{-0.002-0.000-0.011-0.038-0.014}$	m	$1.109^{+0.003+0.011+0.013+0.007+0.022}_{-0.003-0.009-0.015-0.006-0.009}$
	δ	$2.691^{+0.032+0.205+0.099+0.849+0.360}_{-0.032-0.191-0.111-0.664-0.749}$	δ	$1.831^{+0.025+0.088+0.079+0.346+0.251}_{-0.024-0.087-0.086-0.312-0.566}$
	$F_0(0)$	$1.034^{+0.008+0.014+0.035+0.177+0.141}_{-0.008-0.015-0.031-0.154-0.058}$	$F_1(0)$	$1.034^{+0.008+0.014+0.035+0.177+0.141}_{-0.008-0.015-0.031-0.154-0.058}$
$B_c \to B_s$	m	$1.224^{+0.004+0.019+0.009+0.101+0.044}_{-0.004-0.018-0.010-0.081-0.058}$	m	$1.065^{+0.003+0.007+0.010+0.038+0.028}_{-0.003-0.005-0.011-0.032-0.030}$
	δ	$6.005^{+0.092+0.161+0.179+3.239+1.193}_{-0.091-0.149-0.190-1.963-2.141}$	δ	$3.176^{+0.045+0.050+0.099+0.887+0.482}_{-0.044-0.044-0.107-0.673-0.982}$

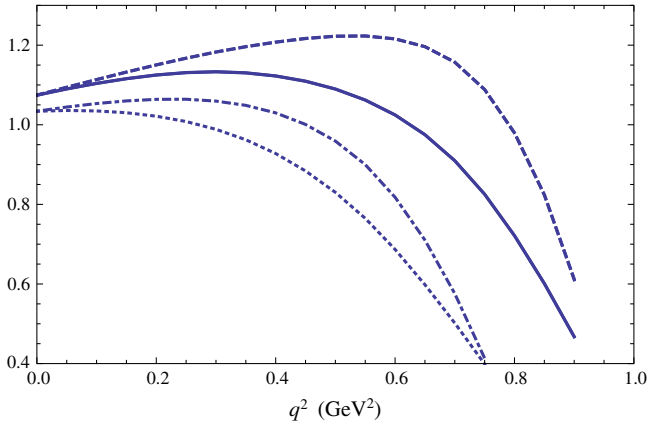

FIG. 3 (color online). The q^2 dependence of the form factor, where the solid, dashed, dotted, and dot-dashed lines denote the $F_0^{B_c\to B_{u,d}}(q^2)$, $F_1^{B_c\to B_{u,d}}(q^2)$, $F_0^{B_c\to B_s}(q^2)$ and $F_1^{B_c\to B_s}(q^2)$, respectively.

contributions to the form factor have the same behavior. This is the QCDF's viewpoint of that the form factor is not fully calculable in the hard scattering picture with the perturbation theory and that the form factor should be regarded as a nonperturbative quantity [31]. From Fig. 4(b) we can see that by keeping the quark transverse momentum k_T, and employing the Sudakov factors to suppress the kinematic configuration when both longitudinal and transverse momentum are soft, the contribution to form factor from $\alpha_s/\pi < 0.3$ region is about 90% and the percentage of contribution from large α_s/π region is small. Our study also shows that besides retaining the quark transverse momentum $k_\perp$ to smear the endpoint divergence behavior and using the Sudakov factor to suppress the nonperturbative contribution in large b region [28], as the discussion in [43], the choice of the hard scale is one of the important ingredients of the pQCD approach, which deserve much attention. If the scale t is chosen as Eq. (C44), then it shows that most of the contributions come from the $\alpha_s/\pi < 0.3$ region, implying that the pQCD approach is applicable to the $B_c \to B$ transition form factors. Of course, there are some controversies, even suspicion, about the suppression mechanism of the Sudakov factor on the nonperturbative contribution, about the choice of the hard scale and so on. The deeper discussion of these problems is needed and should be preformed, but beyond the scope of this paper.

Our numerical results on the branching ratios are given in Table V, where the explanation of uncertainties is the same as that for form factors in Table IV. Following are some comments on the branching ratios.

(i) From Table I, we can see that different branching ratios of $B_c \to BP$, BV decays have been obtained with different approach in previous works, where the same value of coefficient $a_{1,2}$ is taken. The disagreement among previous works is largely originated from the different values of form factor. If the same value of form factors are used, the disparities on branching ratios of a_1-dominated $B_c \to B_{d,s}P$, $B_{d,s}V$ decays will be greatly weakened. For example, if the same $F_0^{B_c\to B_s} = 1.0$ is fixed in the previous works, the branching ratio for $B_c \to B_s\pi$ decays will all be about 10%, which is consistent with our estimation within uncertainties and also agrees with the LHCb measurement [9].

(ii) From Table V, it can be seen that there is a hierarchy between the branching ratios for $B_c \to BP$ and $B_c \to BV$ decays with the same B_q meson in the final state, for example,

$$\mathcal{B}r(B_c \to B_q\pi) > \mathcal{B}r(B_c \to B_q\rho) > \mathcal{B}r(B_c \to B_q\omega), \tag{43}$$

$$\mathcal{B}r(B_c \to B_qK) > \mathcal{B}r(B_c \to B_qK^*), \tag{44}$$

which differs from the previous prediction (see Table I). Two factors had a decisive influence on

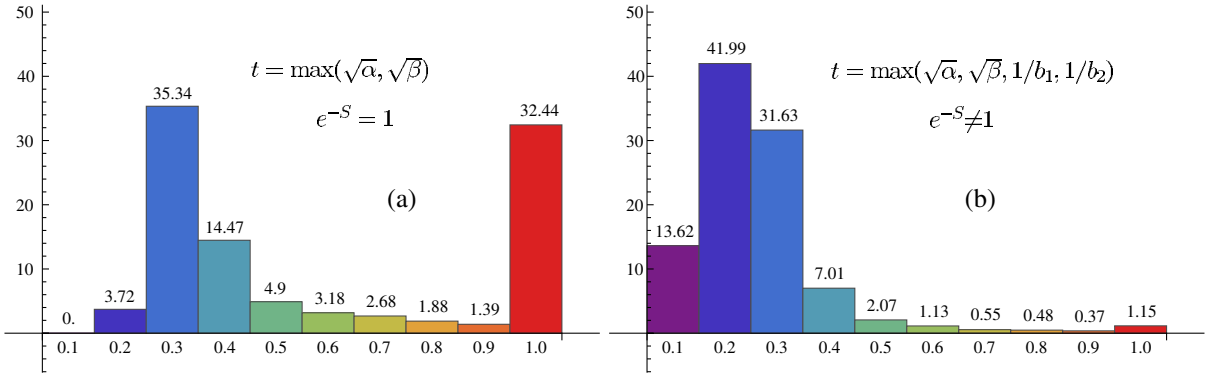

FIG. 4 (color online). The contributions to the form factor $F_0^{B_c\to B_s}(0)$ from different ranges of α_s/π, where the numbers over histogram denote the percentage of the corresponding contributions.

TABLE V. Branching ratio for the $B_c \to BP$, BV decays, where $\mathcal{B}^{t}$ denote the contributions from only the tree operators, $\mathcal{B}^{t+p}$ denote the contributions from both the tree and penguin operators, and $\mathcal{B}^{t+p+a}$ denote the contributions of the tree, penguin, and annihilation topologies; the uncertainties are from mass m_b, m_c, shape parameters ω_{B_c}, ω_{B_q}, and typical scale t, respectively.

Mode	$\mathcal{B}^{t}$	$\mathcal{B}^{t+p}$	$\mathcal{B}^{t+p+a}$
$B_s^0\pi^+$	$8.822^{+0.145+0.120+0.631+3.448+3.178}_{-0.074-0.024-0.526-3.658-1.334} \times 10^{-2}$		
$B_s^0\rho^+$	$3.190^{+0.043+0.041+0.205+1.263+1.123}_{-0.048-0.057-0.192-0.926-0.460} \times 10^{-2}$		
$B_s^0K^+$	$5.237^{+0.037+0.056+0.308+2.133+1.956}_{-0.112-0.056-0.376-1.591-0.794} \times 10^{-3}$	$5.250^{+0.037+0.056+0.310+2.141+1.968}_{-0.111-0.056-0.377-1.595-0.797} \times 10^{-3}$	$5.441^{+0.037+0.057+0.315+2.239+2.019}_{-0.114-0.057-0.384-1.662-0.821} \times 10^{-3}$
$B_s^0K^{*+}$	$9.665^{+0.202+0.200+0.675+3.715+4.775}_{-0.157-0.026-0.594-2.781-1.138} \times 10^{-5}$	$9.671^{+0.199+0.199+0.669+3.719+4.769}_{-0.159-0.031-0.595-2.785-1.142} \times 10^{-5}$	$9.726^{+0.200+0.200+0.674+3.744+4.794}_{-0.159-0.031-0.596-2.803-1.147} \times 10^{-5}$
$B_d^0\pi^+$	$6.850^{+0.080+0.208+0.400+2.511+2.242}_{-0.086-0.207-0.329-1.896-0.901} \times 10^{-3}$	$6.833^{+0.081+0.208+0.401+2.505+2.230}_{-0.085-0.205-0.327-1.890-0.896} \times 10^{-3}$	$6.772^{+0.080+0.207+0.398+2.475+2.215}_{-0.085-0.205-0.326-1.870-0.890} \times 10^{-3}$
$B_d^0\rho^+$	$4.280^{+0.049+0.053+0.251+1.589+1.418}_{-0.054-0.146-0.214-1.186-0.573} \times 10^{-3}$	$4.279^{+0.049+0.053+0.251+1.589+1.417}_{-0.054-0.146-0.214-1.186-0.573} \times 10^{-3}$	$4.253^{+0.049+0.053+0.251+1.576+1.412}_{-0.054-0.145-0.213-1.177-0.570} \times 10^{-3}$
$B_d^0K^+$	$4.370^{+0.051+0.153+0.254+1.496+1.508}_{-0.054-0.152-0.206-1.269-0.595} \times 10^{-4}$		
$B_d^0K^{*+}$	$8.305^{+0.102+0.301+0.494+3.065+2.775}_{-0.100-0.292-0.440-2.266-1.064} \times 10^{-5}$		
$B_u^+\bar{K}^0$	$2.205^{+0.012+0.052+0.138+0.773+2.158}_{-0.019-0.100-0.126-0.694-0.993} \times 10^{-3}$		
$B_u^+\bar{K}^{*0}$	$1.958^{+0.021+0.178+0.235+1.308+2.586}_{-0.036-0.038-0.069-0.520-0.893} \times 10^{-4}$		
$B_u^+\pi^0$	$5.222^{+0.131+0.245+0.140+1.963+4.126}_{-0.034-0.311-0.620-1.724-2.361} \times 10^{-5}$	$5.269^{+0.130+0.245+0.141+2.001+4.094}_{-0.033-0.305-0.615-1.740-2.353} \times 10^{-5}$	$4.924^{+0.123+0.235+0.136+1.877+3.928}_{-0.030-0.291-0.589-1.630-2.232} \times 10^{-5}$
$B_u^+\rho^0$	$1.838^{+0.036+0.169+0.309+1.218+2.294}_{-0.012-0.070-0.028-0.427-0.812} \times 10^{-5}$	$1.840^{+0.036+0.168+0.308+1.218+2.289}_{-0.012-0.067-0.028-0.427-0.811} \times 10^{-5}$	$1.716^{+0.034+0.162+0.297+1.148+2.211}_{-0.010-0.065-0.027-0.393-0.768} \times 10^{-5}$
$B_u^+\omega$	$1.281^{+0.003+0.165+0.215+0.863+1.673}_{-0.010-0.029-0.023-0.385-0.566} \times 10^{-5}$	$1.280^{+0.004+0.166+0.216+0.864+1.681}_{-0.009-0.030-0.024-0.385-0.567} \times 10^{-5}$	$1.371^{+0.005+0.173+0.225+0.916+1.739}_{-0.010-0.031-0.025-0.413-0.598} \times 10^{-5}$
$B_u^+\eta$	$1.417^{+0.039+0.026+0.057+0.456+1.379}_{-0.019-0.040-0.117-0.500-0.698} \times 10^{-4}$	$1.415^{+0.039+0.026+0.057+0.455+1.384}_{-0.019-0.040-0.118-0.501-0.699} \times 10^{-4}$	$0.322^{+0.004+0.016+0.006+0.056+0.244}_{-0.004-0.021-0.040-0.108-0.145} \times 10^{-4}$
$B_u^+\eta'$	$4.183^{+0.339+0.494+0.470+4.165+6.577}_{-0.040-0.420-0.359-2.034-2.414} \times 10^{-6}$	$4.184^{+0.340+0.494+0.470+4.156+6.576}_{-0.039-0.421-0.362-2.017-2.411} \times 10^{-6}$	$7.225^{+0.082+0.356+0.135+1.261+5.465}_{-0.100-0.476-0.895-2.415-3.256} \times 10^{-6}$
$B_u^+K^0$	$6.334^{+0.033+0.151+0.396+2.218+6.196}_{-0.055-0.289-0.362-1.993-2.853} \times 10^{-6}$		
$B_u^+K^{*0}$	$5.622^{+0.061+0.512+0.675+3.759+7.428}_{-0.103-0.108-0.196-1.491-2.563} \times 10^{-7}$		

the above relations. One is kinematic factor. The phase space for $B_c \to BP$ decay is larger than that for $B_c \to BV$ decay, besides the orbital angular momentum $L_{BP} < L_{BV}$. The other is the form factor $F_1^{B_c\to B}(q^2)$. For example, in the previous work [19], the $F_1^{B_c\to B}(q^2)$ goes up along with the growth of q^2, while in this paper, the shape line of $F_1^{B_c\to B}(q^2)$ goes down in large q^2 region. The hierarchy between the branching ratios for $B_c \to BP$ and $B_c \to BV$ decays can be serve as a standard to distinguish different approach, to check the practicality of the pQCD approach.

(iii) As noticed in [27], the contributions of both penguin and annihilation to the branching ratios are very small for $B_c \to BP$, BV decay, because they are seriously suppressed by the CKM factors.

Tree	Penguin	Annihilation
$V_{ud}V_{cs}^* \sim 1$, $V_{us}V_{cs}^* \sim +\lambda$ $V_{ud}V_{cd}^* \sim -\lambda$	$V_{ud}V_{cd}^* + V_{us}V_{cs}^* \sim \lambda^5$	$V_{cb}V_{ub}^* \sim \lambda^5$ $V_{us}V_{cd}^* \sim \lambda^2$,

There are large destructive interferences between the CKM factor $V_{ud}V_{cd}^* \sim -\lambda$ associated to decay amplitude $\mathcal{A}(B_c \to B_u\eta_q)$ and $V_{us}V_{cs}^* \sim +\lambda$ related to decay amplitude $\mathcal{A}(B_c \to B_u\eta_s)$. In addition, the annihilation contribution is proportional to the color-favored tree parameter a_1. Hence, a significant annihilation contribution appear in the $B_c \to B_u\eta^{(\prime)}$ decays.

(iv) As noticed in [27], due to the parameter $a_{1,2}$ and the CKM factors, there is hierarchy of amplitudes among branching ratios for the $B_c \to BP$, BV decays.

Mode	Parameter	CKM factor	Branching ratio
$B_c \to B_s\pi$, $B_s\rho$	a_1	$V_{ud}V_{cs}^* \sim 1$	$\mathcal{O}(10^{-2})$
$B_c \to B_sK^{(*)}$	a_1	$V_{us}V_{cs}^* \sim \lambda$	$10^{-3} \sim 10^{-5}$
$B_c \to B_d\pi$, $B_d\rho$	a_1	$V_{ud}V_{cd}^* \sim \lambda$	$\mathcal{O}(10^{-3})$
$B_c \to B_dK^{(*)}$	a_1	$V_{us}V_{cd}^* \sim \lambda^2$	$10^{-4} \sim 10^{-5}$
$B_c^+ \to B_u^+\bar{K}^{(*)}$	a_2	$V_{ud}V_{cs}^* \sim 1$	$10^{-3} \sim 10^{-4}$
$B_c \to B_u\pi$, $B_u\rho$, $B_u\omega$	a_2	$V_{ud}V_{cd}^* \sim \lambda$	$\mathcal{O}(10^{-5})$
$B_c^+ \to B_u^+K^{(*)}$	a_2	$V_{us}V_{cd}^* \sim \lambda^2$	$10^{-6} \sim 10^{-7}$

Here, the branching ratios for the $B_c \to B_uP$, B_uV decays are larger than those listed in [27]. There are two reasons. One is that the decay amplitudes for the $B_c \to B_uP$, B_uV decays is proportional to parameter a_2, and the value of a_2 in the $\alpha_s/\pi \geq 0.15$ region is much larger than $a_2(m_c)$ used in [27]. The other is that the nonfactorizable contributions $M_{cd,1}^{P,V}$ are always multiplied by the large Wilson coefficient C_1 [see Eqs. (D9)–(D17)], which can largely enhance the branching ratios of color-suppressed tree $B_c \to B_uP$, B_uV decays.

(v) There are large uncertainties to the branching ratios from the shape parameter ω_{B_q} and the scale. Our numerical results are very rough. Despite this, we still get some information about the $B_c \to BP$, BV decays. For example, the branching ratios for

$B_c \to B_{d,s}\pi$, $B_{d,s}\rho$, $B_s K$ are large, these decay modes could clearly be measured by the running LHCb soon.

IV. SUMMARY

In prospects of the potential B_c meson at the LHCb experiments, accurate and thorough studies of the B_c physics will be accessible very soon. In this paper, we calculated the $B_c \to B_{u,d,s}$ transition form factors defined in vector and axial vector currents using the pQCD approach. We find that with appropriate scale, keeping the quark transverse momentum and introducing the Sudakov factors to modify the endpoint behavior, about 90% contributions to the form factors comes form the $\alpha_s/\pi < 0.3$ region. We studied the seventeen exclusive two-body hadronic $B_c \to B_q P$, $B_q V$ decays. It is shown that the contributions of penguin and annihilation to branching ratios are very small, because they relative to the tree contribution are highly suppressed by the CKM factors. The branching ratios for $B_c \to B_{d,s}\pi$, $B_{d,s}\rho$, $B_s K$ are large and could be easily measured by the running LHCb in the near future.

ACKNOWLEDGMENTS

This work is supported by National Natural Science Foundation of China under Grants No. 11147008, No. 11275057, No. 11105043, and No. U1232101). Q. Chang is also supported by Research Fund for the Doctoral Program of Higher Education of China under Grant No. 20114104120002, Foundation for the Author of National Excellent Doctoral Dissertation of P. R. China under Grant No. 201317, and Program for Science and Technology Innovation Talents in Universities of Henan Province.

APPENDIX A: DISTRIBUTION AMPLITUDES OF THE *B* MESON

For the heavy-light B_q meson ($q = u$, d, s), we will adopt the Gaussian type distribution amplitudes proposed in [44],

$$\phi_{B_q}(x,b) = Nx^2\bar{x}^2 \exp\left\{-\frac{1}{2}\left(\frac{xm_{B_q}}{\omega}\right)^2 - \frac{1}{2}\omega^2 b^2\right\}, \quad \text{(A1)}$$

where N is the normalization constant. The shape of the distribution amplitude $\phi_{B_q}(x,0)$ is displayed in Fig. 5. It is easy to see that the large value of shape parameter ω gives a large momentum fraction to the light spectator quark in B_q meson. Because the mass of s quark is heavier than that of u, d quark, it is assumed that the momentum fraction of the spectator quark s in B_s meson should be larger than that of the spectator quark u, d in $B_{u,d}$ meson. In our calculation, we will use $\omega = 0.45 \pm 0.05$ GeV for $B_{u,d}$ meson and $\omega = 0.55 \pm 0.05$ GeV for B_s meson.

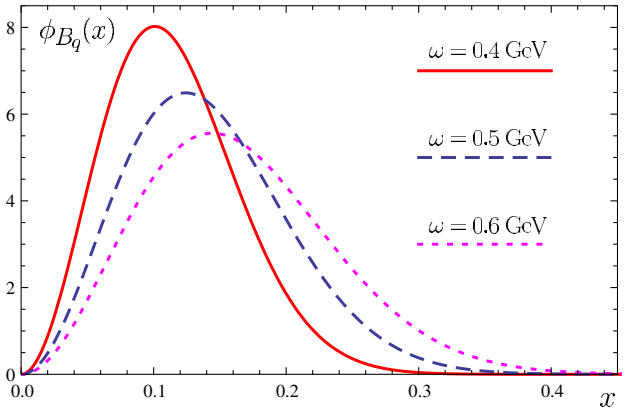

FIG. 5 (color online). B_q meson distribution amplitudes.

Due to the fact $m_{B_c} \approx m_b + m_c$ the B_c meson can be approximated as a non-relativistic bound state of two heavy quark b and c. Its wave function is approximately the solution of the Schrödinger equation with the harmonic oscillator potential. For the ground pseudoscalar B_c meson, the corresponding radial wave function is

$$\psi_{nL}(r) = \psi_{1S}(r) \propto \exp(-\alpha^2 r^2/2), \quad \text{(A2)}$$

where $\alpha^2 = \mu\omega$, the reduced mass $\mu = m_b m_c/(m_b + m_c)$ and the quantum of energy $\omega \approx 0.50 \pm 0.05$ GeV [45].

Applying the Fourier transform, one can get the representation of wave function in momentum space

$$\psi_{1S}(\vec{k}) \sim \int \mathbf{d}\vec{r}\psi_{1S}(r)e^{-i\vec{k}\cdot\vec{r}} \propto \exp(-k^2/2\alpha^2). \quad \text{(A3)}$$

Then adopting the connection [46] between the equal-time prescription in the rest frame and the light-cone dynamics, i.e., assuming that the constituent quarks b and c are on-shell and their light-cone momentum fraction are x_b and x_c, with $x_b + x_c = 1$, one can get the light-cone wave function for B_c meson,

$$\psi_{B_c}(x_i, \vec{k}_\perp) \propto \exp\left\{-\frac{1}{8\alpha^2}\left(\frac{\vec{k}_\perp^2 + m_c^2}{x_c} + \frac{\vec{k}_\perp^2 + m_b^2}{x_b}\right)\right\}. \quad \text{(A4)}$$

The distribution amplitudes of B_c meson is

$$\begin{aligned}\phi_{B_c}(x_i) &= \int \mathbf{d}\vec{k}_\perp \psi_{B_c}(x_i, \vec{k}_\perp) \\ &= N\frac{x_b x_c}{x_b + x_c}\exp\left\{-\frac{1}{8\alpha^2}\left(\frac{m_c^2}{x_c} + \frac{m_b^2}{x_b}\right)\right\}, \quad \text{(A5)}\end{aligned}$$

where N is the normalization constant and the normalization condition is

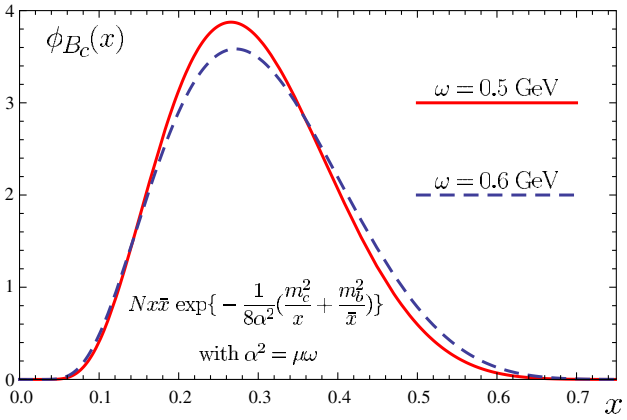

FIG. 6 (color online). B_c meson distribution amplitudes.

$$\int \mathbf{d}x\phi_{B_c}(x) = 1. \tag{A6}$$

In our calculation, $x = x_c$ and $\bar{x} = x_b = 1 - x$, so we have

$$\phi_{B_c}(x) = Nx\bar{x}\exp\left\{-\frac{1}{8\alpha^2}\left(\frac{m_c^2}{x}+\frac{m_b^2}{\bar{x}}\right)\right\}. \tag{A7}$$

The shape of the distribution amplitude of B_c meson is displayed in Fig. 6. It is easy to see that the maximum position is near $m_c/(m_b + m_c)$ and that the small value of parameter ω gives a narrow shape. In our calculation, we will use $\omega = 0.50 \pm 0.05$ GeV for B_c meson.

APPENDIX B: DISTRIBUTION AMPLITUDES OF LIGHT MESONS

The twist-2 quark-antiquark distribution amplitudes of light pseudoscalar and longitudinally polarized vector meson are expressed as [33,47,48],

$$\phi_P^a(x) = 6x\bar{x}\sum_n a_n C_n^{3/2}(\xi), \tag{B1}$$

$$\phi_V(x) = 6x\bar{x}\sum_n a_n^{\parallel} C_n^{3/2}(\xi), \tag{B2}$$

where $C_n^{3/2}(\xi)$ is the Gegenbauer polynomial, and $\xi = x - \bar{x} = 2x - 1$. The Gegenbauer moments $a_0 = 1$ and $a_0^{\parallel} = 1$ due to the normalization condition

$$\int_0^1 \mathbf{d}x\phi_P^a(x) = \int_0^1 \mathbf{d}x\phi_V(x) = 1. \tag{B3}$$

The two-particle twist-3 distribution amplitudes of pseudoscalar meson have the expansion in the terms of the Gegenbauer polynomials [33,47],

$$\phi_P^p(x) = 1 + \left(30\eta_3 - \frac{5}{2}\rho_P^2\right)C_2^{1/2}(\xi) - \left(3\eta_3\omega_3 + \frac{27}{20}\rho_P^2 + \frac{81}{10}\rho_P^2 a_2\right)C_4^{1/2}(\xi), \tag{B4}$$

$$\phi_P^t(x) = C_1^{1/2}(-\xi) + 6\left(5\eta_3 - \frac{1}{2}\eta_3\omega_3 - \frac{7}{20}\rho_P^2 - \frac{3}{5}\rho_P^2 a_2\right)C_3^{1/2}(-\xi). \tag{B5}$$

The expressions of the two-particle twist-3 distribution amplitudes of the longitudinally polarized vector meson are [33,48]

$$\phi_V^t(x) = 3\xi^2, \tag{B6}$$

$$\phi_V^s(x) = -3\xi. \tag{B7}$$

In the mesonic distribution amplitudes, the Gegenbauer polynomials are

$$C_1^{1/2}(x) = x, \tag{B8}$$

$$C_2^{1/2}(x) = \frac{1}{2}(3x^2 - 1), \tag{B9}$$

$$C_3^{1/2}(x) = \frac{1}{2}(5x^3 - 3x), \tag{B10}$$

$$C_4^{1/2}(x) = \frac{1}{8}(35x^4 - 30x^2 + 3), \tag{B11}$$

$$C_1^{3/2}(x) = 3x, \tag{B12}$$

$$C_2^{3/2}(x) = \frac{3}{2}(5x^2 - 1), \tag{B13}$$

$$C_3^{3/2}(x) = \frac{5}{2}(7x^3 - 3x), \tag{B14}$$

$$C_4^{3/2}(x) = \frac{15}{8}(21x^4 - 14x^2 + 1). \tag{B15}$$

APPENDIX C: FORMULA OF DECAY AMPLITUDE

The decay amplitudes can be expressed in terms of the following building block:

$$C_P = \frac{C_F\pi}{N_c} f_{B_c} f_{B_q} f_P, \tag{C1}$$

$$C_V = \frac{C_F\pi}{N_c} f_{B_c} f_{B_q} f_V, \tag{C2}$$

$$iM^P_{a,1} = C_P \int_0^1 \mathbf{d}x_1\mathbf{d}x_2 \int_0^\infty \mathbf{d}b_1\mathbf{d}b_2\phi_{B_c}(x_1)\phi_{B_q}(x_2,b_2)H_a \times \{(m_c - x_2m_2)(m_2u - 2m_1s) + (x_2s + m_3^2)(t - 4m_1m_2)\}, \tag{C3}$$

$$iM^P_{a,2} = -iM^P_{a,2}, \tag{C4}$$

$$iM^P_{a,3} = C_P \int_0^1 \mathbf{d}x_1\mathbf{d}x_2 \int_0^\infty \mathbf{d}b_1\mathbf{d}b_2\phi_{B_c}(x_1)\phi_{B_q}(x_2,b_2)H_a \times 2\mu_P\{(m_c + x_2m_2)(t - 4m_1m_2) + (m_2u - 2m_1s)\}, \tag{C5}$$

$$iM^P_{b,1} = C_P \int_0^1 \mathbf{d}x_1\mathbf{d}x_2 \int_0^\infty \mathbf{d}b_1\mathbf{d}b_2\phi_{B_c}(x_1)\phi_{B_q}(x_2,b_2)H_b \times \{x_1m_1(2m_2u - m_1s) + (x_1u - m_3^2)(t - 4m_1m_2)\}, \tag{C6}$$

$$iM^P_{b,2} = -iM^P_{b,2}, \tag{C7}$$

$$iM^P_{b,3} = C_P \int_0^1 \mathbf{d}x_1\mathbf{d}x_2 \int_0^\infty \mathbf{d}b_1\mathbf{d}b_2\phi_{B_c}(x_1)\phi_{B_q}(x_2,b_2)H_b \times 2\mu_P\{x_1m_1(t - 4m_1m_2) + (2m_2u - m_1s)\}, \tag{C8}$$

$$iM^P_{c,1} = C_P \int_0^1 \mathbf{d}x_1\mathbf{d}x_2\mathbf{d}x_3 \times \int_0^\infty \mathbf{d}b_2\mathbf{d}b_3\phi_{B_c}(x_1)\phi_{B_q}(x_2,b_2)\phi_P^a(x_3)H_c \times \{st(x_1 - x_2) + sm_1m_2(x_2 - x_3) + u(s - m_1m_2)(x_1 - x_3)\}, \tag{C9}$$

$$iM^P_{c,2} = C_P \int_0^1 \mathbf{d}x_1\mathbf{d}x_2\mathbf{d}x_3 \times \int_0^\infty \mathbf{d}b_2\mathbf{d}b_3\phi_{B_c}(x_1)\phi_{B_q}(x_2,b_2)\phi_P^a(x_3)H_c \times \{ut(x_2 - x_1) + um_1m_2(x_1 - x_3) + s(u + m_1m_2)(x_3 - x_2)\}, \tag{C10}$$

$$iM^P_{c,3} = C_P \int_0^1 \mathbf{d}x_1\mathbf{d}x_2\mathbf{d}x_3 \times \int_0^\infty \mathbf{d}b_2\mathbf{d}b_3\phi_{B_c}(x_1)\phi_{B_q}(x_2,b_2)\mu_P H_c \times \{\phi_P^p(x_3)[um_2(x_1 - x_3) + sm_1(x_2 - x_3) + t(m_1 + m_2)(x_1 - x_2)] + \phi_P^t(x_3)2m_1p[m_1(x_1 - x_3) + m_2(x_2 - x_3)]\}, \tag{C11}$$

$$iM^P_{d,1} = C_P \int_0^1 \mathbf{d}x_1\mathbf{d}x_2\mathbf{d}x_3 \times \int_0^\infty \mathbf{d}b_2\mathbf{d}b_3\phi_{B_c}(x_1)\phi_{B_q}(x_2,b_2)\phi_P^a(x_3)H_d \times \{ut(x_2 - x_1) + um_1m_2(x_1 - \bar{x}_3) + s(u + m_1m_2)(\bar{x}_3 - x_2)\}, \tag{C12}$$

$$iM^P_{d,2} = C_P \int_0^1 \mathbf{d}x_1\mathbf{d}x_2\mathbf{d}x_3 \times \int_0^\infty \mathbf{d}b_2\mathbf{d}b_3\phi_{B_c}(x_1)\phi_{B_q}(x_2,b_2)\phi_P^a(x_3)H_d \times \{st(x_1 - x_2) + sm_1m_2(x_2 - \bar{x}_3) + u(s - m_1m_2)(x_1 - \bar{x}_3)\}, \tag{C13}$$

$$iM^P_{d,3} = C_P \int_0^1 \mathbf{d}x_1\mathbf{d}x_2\mathbf{d}x_3 \times \int_0^\infty \mathbf{d}b_2\mathbf{d}b_3\phi_{B_c}(x_1)\phi_{B_q}(x_2,b_2)\mu_P H_d \times \{\phi_P^p(x_3)[um_2(\bar{x}_3 - x_1) + sm_1(\bar{x}_3 - x_2) + t(m_1 + m_2)(x_2 - x_1)] + \phi_P^t(x_3)2m_1p[m_1(x_1 - \bar{x}_3) + m_2(x_2 - \bar{x}_3)]\}, \tag{C14}$$

$$iM^P_{e,1} = C_P \int_0^1 \mathbf{d}x_2\mathbf{d}x_3 \int_0^\infty \mathbf{d}b_2\mathbf{d}b_3\phi_{B_q}(x_2,b_2)H_e \times \{\phi_P^a(x_3)[x_2m_1^2s + \bar{x}_2m_3^3t)] + \mu_P\phi_P^p(x_3)2m_2[x_2t + u]\}, \tag{C15}$$

$$iM^P_{f,1} = C_P \int_0^1 \mathbf{d}x_2\mathbf{d}x_3 \int_0^\infty \mathbf{d}b_2\mathbf{d}b_3\phi_{B_q}(x_2,b_2)H_f \times \{\phi_P^a(x_3)[2m_2m_bu - \bar{x}_3m_1^2s - x_3m_2^2u] + \mu_P\phi_P^p(x_3)[m_bt - 2m_2(t + \bar{x}_3u)] + \mu_P\phi_P^t(x_3)2m_1p[m_b - 2m_2x_3]\}, \tag{C16}$$

$$iM^P_{g,1} = C_P \int_0^1 \mathbf{d}x_1\mathbf{d}x_2\mathbf{d}x_3 \int_0^\infty \mathbf{d}b_1\mathbf{d}b_2\phi_{B_c}(x_1)\phi_{B_q}(x_2,b_2)H_g \times \{\phi_P^a(x_3)[st(\bar{x}_2 - x_3) + tu(x_3 - x_1) - m_1m_bs] + \mu_P\phi_P^p(x_3)m_2[t(\bar{x}_2 - x_1) + u(x_3 - x_1) - 4m_1m_b] + \mu_P\phi_P^t(x_3)2m_1m_2p(x_3 - \bar{x}_2)\}, \tag{C17}$$

$$iM^P_{h,1} = C_P \int_0^1 \mathbf{d}x_1\mathbf{d}x_2\mathbf{d}x_3 \int_0^\infty \mathbf{d}b_1\mathbf{d}b_2\phi_{B_c}(x_1)\phi_{B_q}(x_2,b_2)H_h \times \{\phi_P^a(x_3)[su(\bar{x}_3 - x_2) + tu(x_2 - x_1) + m_1m_cs] + \mu_P\phi_P^p(x_3)m_2[t(x_2 - x_1) + u(\bar{x}_3 - x_1) + 4m_1m_c] + \mu_P\phi_P^t(x_3)2m_1m_2p(x_2 - \bar{x}_3)\}, \tag{C18}$$

$$M^V_{a,1}=C_V m_1 p\int_0^1 \mathbf{d}x_1\mathbf{d}x_2\int_0^\infty \mathbf{d}b_1\mathbf{d}b_2\phi_{B_c}(x_1)\phi_{B_q}(x_2,b_2)H_a \times\{x_2(t+s-4m_1m_2)-2m_c(2m_1-m_2)+2m_3^2\}, \tag{C19}$$

$$M^V_{a,2}=M^V_{a,1}, \tag{C20}$$

$$M^V_{a,3}=0, \tag{C21}$$

$$M^V_{b,1}=C_V m_1 p\int_0^1 \mathbf{d}x_1\mathbf{d}x_2 \times\int_0^\infty \mathbf{d}b_1\mathbf{d}b_2\phi_{B_c}(x_1)\phi_{B_q}(x_2,b_2)H_b \times\{x_1(t-u-4m_1m_2)+2m_3^2\}, \tag{C22}$$

$$M^V_{b,2}=M^V_{b,1}, \tag{C23}$$

$$M^V_{b,3}=0, \tag{C24}$$

$$M^V_{c,1}=C_V m_1 p\int_0^1 \mathbf{d}x_1\mathbf{d}x_2\mathbf{d}x_3 \times\int_0^\infty \mathbf{d}b_2\mathbf{d}b_3\phi_{B_c}(x_1)\phi_{B_q}(x_2,b_2) \times 2\phi_V(x_3)H_c\{(t-m_1m_2)(x_1-x_2)+u(x_1-x_3)\}, \tag{C25}$$

$$M^V_{c,2}=C_V m_1 p\int_0^1 \mathbf{d}x_1\mathbf{d}x_2\mathbf{d}x_3 \times\int_0^\infty \mathbf{d}b_2\mathbf{d}b_3\phi_{B_c}(x_1)\phi_{B_q}(x_2,b_2) \times 2\phi_V(x_3)H_c\{(t-m_1m_2)(x_1-x_2)+s(x_2-x_3)\}, \tag{C26}$$

$$M^V_{c,3}=C_V m_3\frac{f_V^T}{f_V}\int_0^1 \mathbf{d}x_1\mathbf{d}x_2\mathbf{d}x_3 \times\int_0^\infty \mathbf{d}b_2\mathbf{d}b_3\phi_{B_c}(x_1)\phi_{B_q}(x_2,b_2) \times H_c\{\phi_V^t(x_3)2m_1p[m_1(x_3-x_1)+m_2(x_3-x_2)] +\phi_V^s(x_3)[m_2u(x_3-x_1)+m_1s(x_3-x_2) +t(m_1+m_2)(x_2-x_1)]\}, \tag{C27}$$

$$M^V_{d,1}=C_V m_1 p\int_0^1 \mathbf{d}x_1\mathbf{d}x_2\mathbf{d}x_3 \times\int_0^\infty \mathbf{d}b_2\mathbf{d}b_3\phi_{B_c}(x_1)\phi_{B_q}(x_2,b_2) \times 2\phi_V(x_3)H_d\{(t-m_1m_2)(x_2-x_1)+s(\bar{x}_3-x_2)\}, \tag{C28}$$

$$M^V_{d,2}=C_V m_1 p\int_0^1 \mathbf{d}x_1\mathbf{d}x_2\mathbf{d}x_3 \times\int_0^\infty \mathbf{d}b_2\mathbf{d}b_3\phi_{B_c}(x_1)\phi_{B_q}(x_2,b_2) \times 2\phi_V(x_3)H_d\{(t-m_1m_2)(x_2-x_1)+u(\bar{x}_3-x_1)\}, \tag{C29}$$

$$M^V_{d,3}=C_V m_3\frac{f_V^T}{f_V}\int_0^1 \mathbf{d}x_1\mathbf{d}x_2\mathbf{d}x_3 \times\int_0^\infty \mathbf{d}b_2\mathbf{d}b_3\phi_{B_c}(x_1)\phi_{B_q}(x_2,b_2) \times H_d\{\phi_V^t(x_3)2m_1p[m_1(\bar{x}_3-x_1)+m_2(\bar{x}_3-x_2)] +\phi_V^s(x_3)[m_2u(x_1-\bar{x}_3)+m_1s(x_2-\bar{x}_3) +t(m_1+m_2)(x_1-x_2)]\}, \tag{C30}$$

$$M^V_{e,1}=C_V\int_0^1 \mathbf{d}x_2\mathbf{d}x_3\int_0^\infty \mathbf{d}b_2\mathbf{d}b_3\phi_{B_q}(x_2,b_2)H_e \times\left\{\phi_V(x_3)m_1p[x_2(s+t)+2m_3^2] -\phi_V^s(x_3)2m_2m_3\frac{f_V^T}{f_V}(x_2t+u)\right\}, \tag{C31}$$

$$M^V_{f,1}=C_V\int_0^1 \mathbf{d}x_2\mathbf{d}x_3\int_0^\infty \mathbf{d}b_2\mathbf{d}b_3\phi_{B_q}(x_2,b_2)H_f \times\left\{\phi_V(x_3)m_1p[x_3(s+u)+4m_2m_b-2m_1^2] +m_3\frac{f_V^T}{f_V}\phi_V^t(x_3)2m_1p(2m_2x_3-m_b) +m_3\frac{f_V^T}{f_V}\phi_V^s(x_3)[t(2m_2-m_b)+2m_2u\bar{x}_3]\right\}, \tag{C32}$$

$$M^V_{g,1}=C_V\int_0^1 \mathbf{d}x_1\mathbf{d}x_2\mathbf{d}x_3\int_0^\infty \mathbf{d}b_1\mathbf{d}b_2\phi_{B_c}(x_1)\phi_{B_q}(x_2,b_2)H_g \times\left\{\phi_V(x_3)2m_1p[t(\bar{x}_2-x_1)-m_1m_b] +m_2m_3\frac{f_V^T}{f_V}\phi_V^t(x_3)2m_1p(\bar{x}_2-x_3) +m_2m_3\frac{f_V^T}{f_V}\phi_V^s(x_3)[t(x_1-\bar{x}_2)+u(x_1-x_3)+4m_1m_b]\right\}, \tag{C33}$$

$$M^V_{h,1}=C_V\int_0^1\mathbf{d}x_1\mathbf{d}x_2\mathbf{d}x_3\int_0^\infty\mathbf{d}b_1\mathbf{d}b_2\phi_{B_c}(x_1)\phi_{B_q}(x_2,b_2)H_h \times\Big\{\phi_V(x_3)2m_1p[t(x_2-x_1)+s(\bar{x}_3-x_2)+m_1m_c] +m_2m_3\frac{f_V^T}{f_V}\phi_V^t(x_3)2m_1p(\bar{x}_3-x_2) +m_2m_3\frac{f_V^T}{f_V}\phi_V^s(x_3)[t(x_1-x_2)+u(x_1-\bar{x}_3)-4m_1m_c]\Big\}. \tag{C34}$$

The function H_i are defined as

$$H_a = b_1b_2e^{-S_1(t_a)-S_2(t_a)}\alpha_s(t_a)K_0(\sqrt{\alpha_e}b_1) \times\{\theta(b_1-b_2)K_0(\sqrt{\beta_a}b_1)I_0(\sqrt{\beta_a}b_2)+(b_1\leftrightarrow b_2)\}, \tag{C35}$$

$$H_b = b_1b_2e^{-S_1(t_b)-S_2(t_b)}\alpha_s(t_b)K_0(\sqrt{\alpha_e}b_2) \times\{\theta(b_1-b_2)K_0(\sqrt{\beta_b}b_1)I_0(\sqrt{\beta_b}b_2)+(b_1\leftrightarrow b_2)\}, \tag{C36}$$

$$H_{i=c,d} = b_2b_3e^{-S_1(t_i)-S_2(t_i)-S_3(t_i)}\alpha_s(t_i)K_0(\sqrt{\beta_i}b_3) \times\{\theta(b_2-b_3)K_0(\sqrt{\alpha_e}b_2)I_0(\sqrt{\alpha_e}b_3) +(b_2\leftrightarrow b_3)\}_{b_1=b_2}, \tag{C37}$$

$$H_e = b_2b_3e^{-S_2(t_e)-S_3(t_e)}\alpha_s(t_e)K_0(\sqrt{-\alpha_a}b_3) \times\{\theta(b_2-b_3)K_0(\sqrt{-\beta_e}b_2)I_0(\sqrt{-\beta_e}b_3)+(b_2\leftrightarrow b_3)\}, \tag{C38}$$

$$H_f = b_2b_3e^{-S_2(t_f)-S_3(t_f)}\alpha_s(t_f)K_0(\sqrt{-\alpha_a}b_2) \times\{\theta(b_2-b_3)K_0(\sqrt{\beta_f}b_2)I_0(\sqrt{\beta_f}b_3)+(b_2\leftrightarrow b_3)\}, \tag{C39}$$

$$H_{i=g,h} = b_1b_2e^{-S_1(t_i)-S_2(t_i)-S_3(t_i)}\alpha_s(t_i)K_0(\sqrt{\beta_i}b_1) \times\{\theta(b_1-b_2)K_0(\sqrt{-\alpha_a}b_1)I_0(\sqrt{-\alpha_a}b_2) +(b_1\leftrightarrow b_2)\}_{b_2=b_3}. \tag{C40}$$

The exponent of the Sudakov factor e^{-S} is given by

$$S_1(t)=s\left(x_1,b_1,\frac{m_1}{\sqrt{2}}\right)+\frac{5}{3}\int_{1/b_1}^t\frac{\mathbf{d}\mu}{\mu}\gamma_q(\mu), \tag{C41}$$

$$S_2(t)=s(x_2,b_2,q_2^+)+\frac{5}{3}\int_{1/b_2}^t\frac{\mathbf{d}\mu}{\mu}\gamma_q(\mu), \tag{C42}$$

$$S_3(t)=s(x_3,b_3,q_3^+)+s(\bar{x}_3,b_3,q_3^+)+2\int_{1/b_3}^t\frac{\mathbf{d}\mu}{\mu}\gamma_q(\mu), \tag{C43}$$

where the function $s(x,b,Q)$ are defined in Appendix of Ref. [49]. $\gamma_q=-\alpha_s/\pi$ is the quark anomalous dimension.

The hard scale t_i is chosen as the maximum of the virtuality of the internal quark and gluon, including $1/b$ (where b is the transverse separation) i.e.,

$$t_{i=a,b}=\max(\sqrt{\alpha_e},\sqrt{|\beta_i|},1/b_1,1/b_2), \tag{C44}$$

$$t_{i=c,d}=\max(\sqrt{\alpha_e},\sqrt{|\beta_i|},1/b_2,1/b_3), \tag{C45}$$

$$t_{i=e,f}=\max(\sqrt{\alpha_a},\sqrt{|\beta_i|},1/b_2,1/b_3), \tag{C46}$$

$$t_{i=g,h}=\max(\sqrt{\alpha_a},\sqrt{|\beta_i|},1/b_1,1/b_2), \tag{C47}$$

where α_e and α_a are the virtuality of the internal gluon of emission and annihilation diagrams, respectively. The subscript on β_i, the virtuality of the internal quark, corresponds to one index of Fig. 2. Their expressions are

$$\alpha_e=\bar{x}_1\bar{x}_2t-\bar{x}_1^2m_1^2-\bar{x}_2^2m_2^2>0, \tag{C48}$$

$$\alpha_a=x_2\bar{x}_3s+x_2^2m_2^2+\bar{x}_3^2m_3^2>0, \tag{C49}$$

$$\beta_a=\bar{x}_2t-\bar{x}_2^2m_2^2-m_1^2+m_c^2>0, \tag{C50}$$

$$\beta_b=\bar{x}_1t-\bar{x}_1^2m_1^2-m_2^2>0, \tag{C51}$$

$$\beta_c=x_1x_2t+x_1x_3u-x_2x_3s -x_1^2m_1^2-x_2^2m_2^2-x_3^2m_3^2, \tag{C52}$$

$$\beta_d=x_1x_2t+x_1\bar{x}_3u-x_2\bar{x}_3s -x_1^2m_1^2-x_2^2m_2^2-\bar{x}_3^2m_3^2, \tag{C53}$$

$$\beta_e=m_3^2+x_2^2m_2^2+x_2s>0, \tag{C54}$$

$$\beta_f=m_b^2+x_3u-m_1^2-x_3^2m_3^2, \tag{C55}$$

$$\beta_g=x_1\bar{x}_2t+x_1x_3u-\bar{x}_2x_3s +m_b^2-x_1^2m_1^2-\bar{x}_2^2m_2^2-x_3^2m_3^2, \tag{C56}$$

$$\beta_h=x_1x_2t+x_1\bar{x}_3u-x_2\bar{x}_3s+m_c^2 -x_1^2m_1^2-x_2^2m_2^2-\bar{x}_3^2m_3^2. \tag{C57}$$

APPENDIX D: DECAY AMPLITUDES

$$\mathcal{A}(B_c^+\to B_s^0\pi^+)=V_{ud}V_{cs}^*\{a_1M^P_{ab,1}+C_2M^P_{cd,1}\}, \tag{D1}$$

$$\mathcal{A}(B_c^+ \to B_s^0 \rho^+) = V_{ud}V_{cs}^*\{a_1 M_{ab,1}^V + C_2 M_{cd,1}^V\}, \tag{D2}$$

$$\begin{aligned}\mathcal{A}(B_c^+ \to B_s^0 K^+) = {} & V_{us}V_{cs}^*\{a_1 M_{ab,1}^P + C_2 M_{cd,1}^P\} - V_{ub}V_{cb}^*\{(a_4 - a_{10}/2)M_{ab,1}^P + (a_6 - a_8/2)M_{ab,3}^P \\ & + (C_3 - C_9/2)M_{cd,1}^P + (C_5 - C_7/2)M_{cd,3}^P - a_1 M_{ef,1}^P - C_2 M_{gh,1}^P\},\end{aligned} \tag{D3}$$

$$\begin{aligned}\mathcal{A}(B_c^+ \to B_s^0 K^{*+}) = {} & V_{us}V_{cs}^*\{a_1 M_{ab,1}^V + C_2 M_{cd,1}^V\} - V_{ub}V_{cb}^*\{(a_4 - a_{10}/2)M_{ab,1}^V + (C_3 - C_9/2)M_{cd,1}^V \\ & + (C_5 - C_7/2)M_{cd,3}^V - a_1 M_{ef,1}^V - C_2 M_{gh,1}^V\},\end{aligned} \tag{D4}$$

$$\begin{aligned}\mathcal{A}(B_c^+ \to B_d^0 \pi^+) = {} & V_{ud}V_{cd}^*\{a_1 M_{ab,1}^P + C_2 M_{cd,1}^P\} - V_{ub}V_{cb}^*\{(a_4 - a_{10}/2)M_{ab,1}^P + (a_6 - a_8/2)M_{ab,3}^P + (C_3 - C_9/2)M_{cd,1}^P \\ & + (C_5 - C_7/2)M_{cd,3}^P - a_1 M_{ef,1}^P - C_2 M_{gh,1}^P\},\end{aligned} \tag{D5}$$

$$\begin{aligned}\mathcal{A}(B_c^+ \to B_d^0 \rho^+) = {} & V_{ud}V_{cd}^*\{a_1 M_{ab,1}^V + C_2 M_{cd,1}^V\} - V_{ub}V_{cb}^*\{(a_4 - a_{10}/2)M_{ab,1}^V + (C_3 - C_9/2)M_{cd,1}^V \\ & + (C_5 - C_7/2)M_{cd,3}^V - a_1 M_{ef,1}^V - C_2 M_{gh,1}^V\},\end{aligned} \tag{D6}$$

$$\mathcal{A}(B_c^+ \to B_d^0 K^+) = V_{us}V_{cd}^*\{a_1 M_{ab,1}^P + C_2 M_{cd,1}^P\}, \tag{D7}$$

$$\mathcal{A}(B_c^+ \to B_d^0 K^{*+}) = V_{us}V_{cd}^*\{a_1 M_{ab,1}^V + C_2 M_{cd,1}^V\}, \tag{D8}$$

$$\mathcal{A}(B_c^+ \to B_u^+ \bar{K}^0) = V_{ud}V_{cs}^*\{a_2 M_{ab,1}^P + C_1 M_{cd,1}^P\}, \tag{D9}$$

$$\mathcal{A}(B_c^+ \to B_u^+ \bar{K}^{*0}) = V_{ud}V_{cs}^*\{a_2 M_{ab,1}^V + C_1 M_{cd,1}^V\}, \tag{D10}$$

$$\mathcal{A}(B_c^+ \to B_u^+ K^0) = V_{us}V_{cd}^*\{a_2 M_{ab,1}^P + C_1 M_{cd,1}^P\}, \tag{D11}$$

$$\mathcal{A}(B_c^+ \to B_u^+ K^{*0}) = V_{us}V_{cd}^*\{a_2 M_{ab,1}^V + C_1 M_{cd,1}^V\}, \tag{D12}$$

$$\begin{aligned}\sqrt{2}\mathcal{A}(B_c^+ \to B_u^+ \pi^0) = {} & -V_{ud}V_{cd}^*\{a_2 M_{ab,1}^P + C_1 M_{cd,1}^P\} - V_{ub}V_{cb}^*\Big\{-a_1 M_{ef,1}^P - C_2 M_{gh,1}^P \\ & + \left(a_4 + a_{10} + \frac{3}{2}a_9\right)M_{ab,1}^P + \frac{3}{2}a_7 M_{ab,2}^P + (a_6 + a_8)M_{ab,3}^P \\ & + \left(C_3 + C_9 + \frac{3}{2}C_{10}\right)M_{cd,1}^P + \frac{3}{2}C_8 M_{cd,2}^P + (C_5 + C_7)M_{cd,3}^P\Big\},\end{aligned} \tag{D13}$$

$$\begin{aligned}\sqrt{2}\mathcal{A}(B_c^+ \to B_u^+ \rho^0) = {} & -V_{ud}V_{cd}^*\{a_2 M_{ab,1}^V + C_1 M_{cd,1}^V\} - V_{ub}V_{cb}^*\Big\{(C_5 + C_7)M_{cd,3}^V \\ & - a_1 M_{ef,1}^V + \left(a_4 + a_{10} + \frac{3}{2}a_9\right)M_{ab,1}^V + \frac{3}{2}a_7 M_{ab,2}^V \\ & - C_2 M_{gh,1}^V + \left(C_3 + C_9 + \frac{3}{2}C_{10}\right)M_{cd,1}^V + \frac{3}{2}C_8 M_{cd,2}^V\Big\},\end{aligned} \tag{D14}$$

$$\begin{aligned}\sqrt{2}\mathcal{A}(B_c^+ \to B_u^+ \omega) = {} & V_{ud}V_{cd}^*\{a_2 M_{ab,1}^V + C_1 M_{cd,1}^V\} - V_{ub}V_{cb}^*\{(C_5 + C_7)M_{cd,3}^V + (2a_3 + a_4 + a_9/2 + a_{10})M_{ab,1}^V \\ & + (2a_5 + a_7/2)M_{ab,2}^V + (C_3 + 2C_4 + C_9 + C_{10}/2)M_{cd,1}^V + (2C_6 + C_8/2)M_{cd,2}^V \\ & - a_1 M_{ef,1}^V - C_2 M_{gh,1}^V\},\end{aligned} \tag{D15}$$

$$\begin{aligned}\sqrt{2}\mathcal{A}(B_c^+ \to B_u^+ \eta_q) = {} & V_{ud}V_{cd}^*\{a_2 M_{ab,1}^P + C_1 M_{cd,1}^P\} - V_{ub}V_{cb}^*\{-a_1 M_{ef,1}^P - C_2 M_{gh,1}^P + (2a_3 + a_4 + a_9/2 + a_{10})M_{ab,1}^P \\ & + (2a_5 + a_7/2)M_{ab,2}^P + (C_3 + 2C_4 + C_9 + C_{10}/2)M_{cd,1}^P + (2C_6 + C_8/2)M_{cd,2}^P \\ & + (a_6 + a_8)M_{ab,3}^P + (C_5 + C_7)M_{cd,3}^P\}.\end{aligned} \tag{D16}$$

$$\mathcal{A}(B_c^+ \to B_u^+ \eta_s) = V_{us}V_{cs}^*\{a_2 M_{ab,1}^P + C_1 M_{cd,1}^P\} - V_{ub}V_{cb}^*\left\{\left(a_3 - \frac{1}{2}a_9\right)M_{ab,1}^P + \left(a_5 - \frac{1}{2}a_7\right)M_{ab,2}^P + \left(C_4 - \frac{1}{2}C_{10}\right)M_{cd,1}^P + \left(C_6 - \frac{1}{2}C_8\right)M_{cd,2}^P\right\}, \tag{D17}$$

$$\mathcal{A}(B_c^+ \to B_u^+ \eta) = \cos\phi\mathcal{A}(B_c^+ \to B_u^+ \eta_q) - \sin\phi\mathcal{A}(B_c^+ \to B_u^+ \eta_s), \tag{D18}$$

$$\mathcal{A}(B_c^+ \to B_u^+ \eta') = \sin\phi\mathcal{A}(B_c^+ \to B_u^+ \eta_q) + \cos\phi\mathcal{A}(B_c^+ \to B_u^+ \eta_s), \tag{D19}$$

[1] J. Beringer *et al.* (Particle Data Group), Phys. Rev. D **86**, 010001 (2012).
[2] F. Abe *et al.* (CDF Collaboration), Phys. Rev. D **58**, 112004 (1998); Phys. Rev. Lett. **81**, 2432 (1998).
[3] T. Aaltonen *et al.* (CDF Collaboration), Phys. Rev. Lett. **100**, 182002 (2008).
[4] R. Aaij *et al.* (LHCb Collaboration), Phys. Rev. Lett. **109**, 232001 (2012).
[5] R. Aaij *et al.* (LHCb Collaboration), Eur. Phys. J. C **74**, 2839 (2014).
[6] M. Lusignoli and M. Masetti, Z. Phys. C **51**, 549 (1991).
[7] C. Chang and Y. Chen, Phys. Rev. D **49**, 3399 (1994).
[8] M. Beneke and G. Buchalla, Phys. Rev. D **53**, 4991 (1996); C.-H. Chang, S.-L. Chen, T.-F. Feng, and X.-Q. Li, Phys. Rev. D **64**, 014003 (2001); Commun. Theor. Phys. **35**, 57 (2001).
[9] R. Aaij *et al.* (LHCb Collaboration), Phys. Rev. Lett. **111**, 181801 (2013).
[10] N. Brambilla *et al.* (Quarkonium Working Group), arXiv: hep-ph/0412158.
[11] V. Abazov *et al.* (D0 Collaboration), Phys. Rev. Lett. **101**, 012001 (2008).
[12] R. Aaij *et al.* (LHCb Collaboration), Phys. Rev. D **87**, 071103 (2013).
[13] R. Aaij *et al.* (LHCb Collaboration), Phys. Rev. D **87**, 112012 (2013).
[14] R. Aaij *et al.* (LHCb Collaboration), J. High Energy Phys. 11 (2013) 094.
[15] R. Aaij *et al.* (LHCb Collaboration), Phys. Rev. Lett. **108**, 251802 (2012).
[16] A. Abulencia *et al.* (CDF Collaboration), Phys. Rev. Lett. **97**, 012002 (2006).
[17] S. Descotes-Genon, J. He, E. Kou, and P. Robbe, Phys. Rev. D **80**, 114031 (2009); X. Liu, Z. Xiao, and C. Lü, Phys. Rev. D **81**, 014022 (2010); Y. Yang, J. Sun, and N. Wang, Phys. Rev. D **81**, 074012 (2010).
[18] A. Likhoded and A. V. Luchinsky, Phys. Rev. D **82**, 014012 (2010); I. P. Gouz, V. V. Kiselev, A. K. Likhoded, V. I. Romanovsky, and O. P. Yushchenko, Phys. At. Nucl. **67**, 1559 (2004); V. Kiselev, arXiv:hep-ph/0211021.
[19] S. Naimuddin, S. Kar, M. Priyadarsini, N. Barik, and P. C. Dash, Phys. Rev. D **86**, 094028 (2012).
[20] H. Choi and C. Ji, Phys. Rev. D **80**, 114003 (2009).
[21] E. Hernández, J. Nieves, and J. Verde-Velasco, Phys. Rev. D **74**, 074008 (2006).
[22] M. Ivanov, J. Körner, and P. Santorelli, Phys. Rev. D **73**, 054024 (2006); **63**, 074010 (2001).
[23] D. Ebert, R. Faustov, and V. Galkin, Eur. Phys. J. C **32**, 29 (2003).
[24] A. El-Hady, J. Munoz, and J. Vary, Phys. Rev. D **62**, 014019 (2000).
[25] D. Du and Z. Wang, Phys. Rev. D **39**, 1342 (1989).
[26] P. Colangelo and F. Fazio, Phys. Rev. D **61**, 034012 (2000).
[27] J. Sun, Y. Yang, W. Du, and H. Ma, Phys. Rev. D **77**, 114004 (2008).
[28] C. Chang and H. Li, Phys. Rev. D **55**, 5577 (1997); T. Yeh and H. Li, Phys. Rev. D **56**, 1615 (1997); Y. Keum, H. Li, and A. Sanda, Phys. Lett. B **504**, 6 (2001); Y. Keum and H. Li, Phys. Rev. D **63**, 074006 (2001); C. Lü, K. Ukai, and M. Yang, Phys. Rev. D **63**, 074009 (2001); C. Lü and M. Yang, Eur. Phys. J. C **23**, 275 (2002).
[29] For a review, see G. Buchalla, A. Buras, and M. Lautenbacher, Rev. Mod. Phys. **68**, 1125 (1996); or A. J. Buras, arXiv:hep-ph/9806471.
[30] G. Lepage and S. Brodsky, Phys. Rev. D **22**, 2157 (1980).
[31] M. Beneke, G. Buchalla, M. Neubert, and C. Sachrajda, Phys. Rev. Lett. **83**, 1914 (1999); Nucl. Phys. **B591**, 313 (2000); **B606**, 245 (2001); D. Du, D. Yang, and G. Zhu, Phys. Lett. B **488**, 46 (2000); **509**, 263 (2001); Phys. Rev. D **64**, 014036 (2001).
[32] C. Bauer, S. Fleming, and M. Luke, Phys. Rev. D **63**, 014006 (2000); C. W. Bauer, S. Fleming, D. Pirjol, and I. W. Stewart, Phys. Rev. D **63**, 114020 (2001); C. Bauer and I. Stewart, Phys. Lett. B **516**, 134 (2001); C. Bauer, D. Pirjol, and I. Stewart, Phys. Rev. D **65**, 054022 (2002); C. W. Bauer, S. Fleming, D. Pirjol, I. Z. Rothstein, and I. W. Stewart, Phys. Rev. D **66**, 014017 (2002); M. Beneke, A. P. Chapovsky, M. Diehl, and Th. Feldmann, Nucl. Phys. **B643**, 431 (2002); M. Beneke and T. Feldmann, Phys. Lett. B **553**, 267 (2003); Nucl. Phys. **B685**, 249 (2004).
[33] T. Kurimoto, H. Li, and A. Sanda, Phys. Rev. D **65**, 014007 (2001).
[34] M. Wirbel, B. Stech, and M. Bauer, Z. Phys. C **29**, 637 (1985).
[35] Th. Feldmann, P. Kroll, and B. Stech, Phys. Rev. D **58**, 114006 (1998).

[36] A. Ali, G. Kramer, Y. Li, C. Lü, Y. L. Shen, W. Wang, and Y. M. Wang, Phys. Rev. D **76**, 074018 (2007).
[37] R. Escribano and J. Nadal, J. High Energy Phys. 05 (2007) 006; F. Ambrosino *et al.* (KLOE Collaboration), J. High Energy Phys. 07 (2009) 105.
[38] W.-F. Wang, Y.-Y. Fan, M. Liu, and Z.-J. Xiao, Phys. Rev. D **87**, 097501 (2013); Y. Charng, T. Kurimoto, and H.-n. Li, Phys. Rev. D **74**, 074024 (2006).
[39] S. Aoki *et al.* (FLAG Working Group), arXiv:1310.8555.
[40] P. Ball and G. Jones, J. High Energy Phys. 03 (2007) 069.
[41] T.-W. Chiu, T.-H. Hsieh, C.-H. Huang, and K. Ogawa (TWQCD Collaboration), Phys. Lett. B **651**, 171 (2007).
[42] P. Ball, V. Braun, and A. Lenz, J. High Energy Phys. 05 (2006) 004.
[43] C. Lü and M. Yang, Eur. Phys. J. C **28**, 515 (2003).
[44] Y. Keum, H. Li, and A. Sanda, Phys. Rev. D **63**, 054008 (2001).
[45] D. Ebert, R. Faustov, and V. Galkin, Eur. Phys. J. C **71**, 1825 (2011); B. Patel, and P. Vinodkumar, J. Phys. G **36**, 035003 (2009) and references therein.
[46] G. Lepage, and S. Brodsky, Phys. Rev. D **22**, 2157 (1980); T. Huang, B. Ma, and Q. Shen, Phys. Rev. D **49**, 1490 (1994).
[47] P. Ball, J. High Energy Phys. 01 (1999) 010.
[48] P. Ball, V. M. Braun, Y. Koike, and K. Tanaka, Nucl. Phys. **B529**, 323 (1998).
[49] H. Li, Phys. Rev. D **52**, 3958 (1995).